Dolomite dissolution in aqueous solutions in the presence of nucleotides and their structural components at 25°C and pCO_2 ~ 1 atm.

Sanoopkumar Puthiya Veetil[a], Alfonso Mucci*[a] and Takeshi Arakaki[b]

a – GEOTOP and Department of Earth and Planetary Sciences, McGill University, Montreal, QC, H3A 0E8, Canada

b- Faculty of Economics, Okinawa International University, Okinawa 901-2701, Japan

*Corresponding author email: alfonso.mucci@mcgill.ca

Published in Chemical Geology:

PUTHIYA VEETIL S.K., MUCCI A. and ARAKAKI T. (2017) Dolomite dissolution in aqueous solutions in the presence of nucleotides and their structural components at 25°C and pCO_2 ~ 1 atm. Chemical Geology **465:** 64-74. http://dx.doi.org/10.1016/j.chemgeo.2017.05.022

Abstract

The kinetics and stoichiometry of dolomite dissolution were investigated in deionized water at 25°C and pCO_2 ~1 atm in the absence (control) and presence of various nucleotides and their structural components at low concentrations (1mM). Dissolutions were conducted in "free-drift" mode and rates estimated based on the accumulation rate of calcium and magnesium ions in solution. The additives considered in this study are likely present at low concentrations (< mM) in deep, carbonate aquifers targeted for CO_2 geological sequestration. Results of our control experiment are consistent with rates and stoichiometries reported in earlier studies. In the presence of nucleotides, dolomite dissolution was inhibited and proceeded incongruently, yielding a Mg:Ca solution ratio ≥2. An investigation of the nucleotide structural components (nucleosides, nitrogenous bases and phosphates) revealed that, whereas they nearly all inhibited dolomite dissolution, only phosphate salts (mono-, di-, tri-, and hexametaphosphate) lead to incongruent dissolution. Examination of the surface morphology and phosphate analysis of the solids reacted in the presence of nucleotides and phosphate salts revealed the formation of a solid phosphate phase on the dolomite surface, likely a Ca rich-phosphate phase that accounts for the observed dissolution incongruency.

Keywords: Dolomite; CO_2 sequestration; nucleotides; phosphates; incongruent dissolution

1. Introduction

Carbonate reservoirs are hosts to more than 50% of the world's hydrocarbon reserves (Saberi, 2010). The Western Canadian sedimentary basin (central Alberta and southwest Alberta and Manitoba) comprises a number of ancient carbonate reefs, many of which have been partially or fully dolomitized, and these account for a substantial percentage of oil (50.7%) and gas (23%) producing reservoirs (Creaney and Allan, 1990; Fowler et al., 2001; Halbertsma, 1994; Hamilton and Olson, 1990; Hay, 1994). In many cases, the porosity and permeability of these reservoirs was acquired as a result of dolomitization (Qing and Mountjoy, 1992; Sharma et al., 2014) and are now identified as potential sites for geological sequestration of CO_2 (Bachu, 2003; Bachu and Adams, 2003; Bachu and Stewart, 2002). The injection and dissolution of CO_2 in these reservoirs will lower the pH of the reservoir fluids and promote the dissolution of surrounding carbonate minerals (André et al., 2007; André et al., 2010; Garcia et al., 2011; Hao et al., 2013; Luquot and Gouze, 2009; Mohamed et al., 2011; Tutolo et al., 2014). The dissolution and precipitation of carbonate minerals in aqueous solutions at high CO_2 partial pressures is of growing research interest in the context of the geological sequestration of CO_2 in deep aquifers (Oelkers et al., 2011; Oelkers and Schott, 2005; Wellman et al., 2003).

Dolomite is a double carbonate, in which the cationic layer alternately hosts calcium and magnesium ions (Morse et al., 2007; Warren, 2000). Dolomite is abundant in ancient rocks, fossil carbonate reefs, but rare in modern sedimentary deposits (Arvidson and Mackenzie, 1999; McKenzie and Vasconcelos, 2009; Warren, 2000). A large number of studies have been carried out to determine the kinetics of dolomite dissolution in aqueous solutions in an effort to identify factors that control the reaction (Busenberg and Plummer, 1982; Pokrovsky and Schott, 2001; Sherman and Barak, 2000; Lüttge et al., 2003; Urosevic et al., 2012), more recently in the context

of geological CO_2 sequestration and the structural integrity of limestone reservoirs (Gautelier et al., 2007; Luhmann et al., 2014; Pokrovsky et al., 2009a; Pokrovsky et al., 2005; Pokrovsky et al., 2009b), but also in an attempt to resolve the mysteries of its formation at low temperatures (Busenberg and Plummer, 1982; Chou et al., 1989; Gautelier et al., 1999; Herman, 1982; Herman and White, 1985; Morse and Arvidson, 2002; Morse et al., 2007; Orton and Unwin, 1993; Pokrovsky et al., 1999).

McKenzie et al. (2009) recently reported that bacteria can promote the precipitation of dolomite. Bacteria and their metabolic products are ubiquitous in subaqueous environments (Dhami et al., 2013; Gray and Engel, 2013; Paul, 2014) and the former can thrive in carbonate (calcite and dolomite) hydrocarbon-bearing reservoirs (Machel et al., 1995; Wolicka et al., 2010). Hence, these reservoir rocks and associated fluids may contain bioactive molecules such as nucleotides (Bulleid, 1978; Holm Hansen and Booth, 1966; Karl and Craven, 1980; Oomori and Kitano, 1991; Webster et al., 1984) that may influence the dissolution and growth of carbonate minerals (calcite and dolomite) in these environments. Numerous studies have been conducted to determine the effects of temperature, pH, salinity and pCO_2 on the dissolution of Ca and Mg carbonates (Chou et al., 1989; Pokrovsky et al., 2005; Pokrovsky et al., 2009b; Zhang et al., 2007), but few have focused on the influence of organic ligands on the reaction (Jordan et al., 2007; Oelkers et al., 2011; Pokrovsky et al., 2009a). Meyer (1984) reported on the influence of several additives, including nucleotides (ATP and ADP), on calcite growth rates from aqueous solutions. His results show an inhibition of calcite growth upon an increase in additive concentration, but no study of the influence of nucleotides on carbonate dissolution kinetics has been conducted to date. The present study strives to partially fill this gap by reporting the results of an experimental study of the kinetics and stoichiometry of dolomite dissolution in the absence (control) and presence of

four nucleotides (ATP, ADP, GDP and AMP) and their structural components (nucleosides, purines, sugars and phosphate backbone). Experiments were carried out in deionized water at a CO_2 partial pressure of one atmosphere in order to identify the chemical constituents responsible for the inhibitory and incongruent dissolution of the mineral that we observed in the presence of the nucleotides.

2. Materials and Methods

2.1. Sample characteristics

Dolomite crystals (hydrothermal, from Franklin, Sussex County, NJ, U.S.A.), purchased from Boreal Science, were used in all experiments. The material was crushed, ground in an agate mortar and pestle, and sized by dry sieving between 149-212 μm. The sized material was washed 5 minutes in a 0.05N hydrochloric acid (HCl) solution to remove fine particles and impurities, separated from the solution by filtration through a 0.45 μm Millipore polycarbonate filter, rinsed five times with deionized water, and allowed to dry at room temperature. The geometric surface area of the ground material was estimated at 155 cm^2/g based on the mean grain size (180.5 μm) and the correlation published by Plummer and Wigley (1976) for particles sized between 20-325 mesh. The mineralogy of the material was characterized by X-ray diffraction (XRD) (Rigaku Smartlab: Cu Kα anode at 44 mA, 2θ step size of 0.01 degree and scan speed of 1.5 deg/min) whereas its metal (Ca, Mg, Fe, Mn, Na and Sr) content (Table 1) was determined by Flame Atomic Absorption/Emission Spectrometry (AAS) (Perkin Elmer Analyst 100 Atomic Absorption Spectrometer) following dissolution of a known weight of the material in 5N HCl and further dilution in 0.1N HCl. The AAS was calibrated using external standards prepared by dilution, in 0.1N HCl, of commercially purchased 1000 ppm certified solutions. The results of the AAS and

XRD analyses revealed that the sample is a calcium-rich dolomite having 56.7 % $CaCO_3$ and 43.3% $MgCO_3$ (CaO- 31.8% and MgO-20.9%) with less than 5% $FeCO_3$. The excess calcium in the dolomite can be explained by the presence of a ferroan dolomite (ankerite) that we identified by XRD Rietveld analysis (Chai et al., 1995).

2.2. General Procedure

The dolomite dissolution rate measurements were carried out in "free-drift" mode at 25^0C, 1 atm CO_2 partial pressure in a 500 mL jacketed reaction vessel. The experimental set-up is schematically represented in Fig.1. Temperature was maintained constant by recirculating water through the jacketed vessel from a water bath set at 25.0 ± 0.1°C. The reaction vessel was fitted with a PVC lid with holes for insertion of a Teflon stirring impeller, CO_2 gas dispersion tube and pH combination electrode. The impeller was driven by an overhead motor at a stirring speed of 120 rpm, high enough to keep the solid particles in suspension.

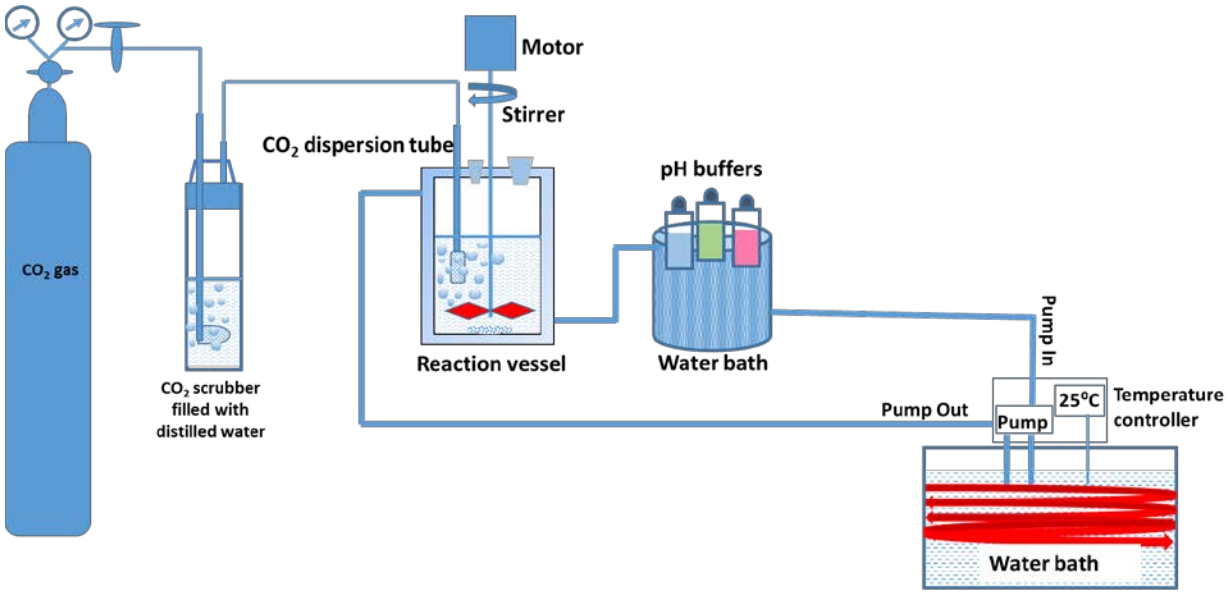

101

102 **Fig.1** Schematic representation of the experimental design of the dolomite dissolution experiment.

103

The dissolution experiments were carried out in 300 mL of deionized water in the absence (control experiment) and presence of selected additives (Table 2) at an initial concentration of 1 mM. The additives were chosen because of their potential presence in natural sedimentary environments and their ability to complex divalent cations. The initial pH of the solution was adjusted between 4-5 using standardized HCl (0.1M) or NaOH (1M) solutions. Commercial grade CO_2 (100%) was pre-saturated with water by bubbling the gas through a scrubber filled with deionized water before being channeled into the reaction vessel through a fritted dispersion tube. The gas flow was set at approximately 75 mL/min, thus maintaining the CO_2 partial pressure in solution at ~0.97 atm, as estimated from pH measurements in pure water. The solution was pre-equilibrated with the CO_2 gas for 6 hours or until a steady-state pH was reached. The dissolution experiment was initiated upon the addition of a weighed amount (~0.5g) of the sized dolomite crystals to the reaction vessel. Less than 10% of the starting material was dissolved by the end of each experiment so that variations in surface area were estimated at less than 14% and deemed to have a small influence on the measured rates. The pH was measured using a combination glass electrode (Radiometer® GK2491C) connected to a Radiometer® M84 pH/millivolt-meter (Radiometer Copenhagen PHM 84 Research pH Meter). The pH electrode was calibrated using three NIST-traceable buffers (Fisher Scientific; pH = 2.00, 4.00 and 7.00 at 25°C), prior to and after each sample measurement. Aliquots (10 mL) of the reacting solution were taken at the beginning of the run and at ~24-hour intervals over the next five days (total of 5 sampling intervals for each experiment, time intervals between samplings sometime differ because of statutory holidays and lock-down of the laboratories, see Appendix A-1). The aliquots were filtered through a 0.45 μm Millipore polycarbonate filter and acidified with 0.1 mL of 5N HCl. Dissolved Ca, Mg, Fe and Mn were analyzed by AAS and Na by Atomic Emission Spectroscopy (AES). The detection

limits were estimated at 0.04 mg/L for Ca, Mg, Fe, and Mn and 0.01 mg/L for Na. The pH of the reacting solution was noted at each sampling interval. The initial and final pH for all experiments are given in Appendix (Table A-1).

2.3. Experimental calculations

The pH and pCO_2 were used to calculate the carbonic acid speciation (carbonate and bicarbonate ion concentrations) of the reacting solutions at different time intervals by simple iterative mathematical calculations. The thermodynamic constants used in the speciation and saturation calculations were taken from the WATEQ4F database file in the PHREEQC program provided by the USGS (Parkhurst and Appelo, 2011). The additive species and complexation constants considered in the equilibrium calculations are given in Table 2. The activity coefficients of charged species were estimated using an extended Debye-Hückel equation whereas those of neutral species were calculated according to: $\gamma = 10^{-0.5I}$ (Busenberg and Plummer, 1982).

The dissolution rate was calculated from the change in total dissolved Ca^{2+} or Mg^{2+} concentration (in mol/l), $\Delta[Ca^{2+}]$ or $\Delta[Mg^{2+}]$, according to Equation (1):

$$R\ (\text{mmol}\,\text{cm}^{-2}\ \text{s}^{-1}) = \frac{\Delta[\text{Me}]}{\Delta t} \text{ x } \frac{V}{S} \qquad (1)$$

where Δt is the elapsed time in seconds, [Me] is total Ca or Mg concentration, V is the volume of the solution (mL) and, S is the total surface area of the dolomite crystals (cm^2). The dissolution rates were corrected for evaporation, as determined from the change in the chloride concentration of a 0.1N NaCl solution under the same experimental conditions (temperature, stirring and

bubbling). The chloride concentration was measured using a Radiometer Titralab 865 automated potentiometric titrator connected to a Ag electrode and a $Hg/HgSO_4$ reference electrode. The cumulative evaporation after 7 days was on the order of 0.7%, negligible relative to the analytical uncertainty of the Ca^{2+} and Mg^{2+} analyses.

3. Result and Discussion

3.1. Influence of nucleotides on dolomite dissolution

Results of the "free-drift", dolomite dissolution experiments performed in the absence (control) and presence (1 mM) of the selected nucleotides at 25^0C and 1 atm CO_2 partial pressure are presented in Figs. 2 and 3. Our results are also compared to those of Busenberg and Plummer (1982) obtained by monitoring the weight loss of single crystals of sedimentary and hydrothermal dolomite in "free drift" mode. Results of our control experiment are compatible with those of Busenberg and Plummer (1982) for their hydrothermal dolomite. The small rate discrepancies could be attributed to differences in the stability of the dolomite materials as well as the methods used to estimate the rates. On the other hand, our rates are significantly faster than those obtained from the vertical scanning interferometer study conducted by Lüttge et al. (2003) on various cleavage faces of a dolomite single crystal in 0.001M HCl solutions (pH ~3). The authors offer a number of reasons why this is so, including the highly reactive surface area and etch pit dominated kinetics of mineral powders. Results of experimental studies of dolomite dissolution must obviously be carefully scrutinized and extrapolated to natural settings with caution.

The presence of nucleotides clearly leads to significant inhibition of the dolomite dissolution rate, as tracked by the release of calcium to the solution. In all cases, the rate of dissolution decreases exponentially with increasing pH of the solution. Similar trends were

reported in CO_2-rich solutions (pCO_2~1atm), in which the rate of dolomite dissolution decreased sharply with increasing pH above 5.5 (Busenberg and Plummer, 1982; Herman and White, 1985; Pokrovsky and Schott, 2001; Pokrovsky et al., 1999; Urosevic et al., 2012). Results of our dolomite dissolution experiments (Fig. 2) also display features that are similar to those observed by Plummer et al. (1978) for calcite dissolution in "pH stat" and "free drift" experiments at various pCO_2. Plummer et al. (1978) divided their log (rate) vs pH plot into three regions: a linear region, far from equilibrium, where dissolution mostly depends on pH, a region where rates vary with both pH and pCO_2, and a region characterized by a sharp inflection in the curve (i.e., rapid reduction in the rate). In the latter region, calcite and dolomite dissolution is slow and was reported to vary linearly with the bicarbonate ion activity ($aHCO_3^-$) in solution at a given pCO_2 (Busenberg and Plummer, 1982; Plummer et al., 1978). The boundaries between the regions is a function of the pCO_2 and reaction progress. (Plummer et al., 1978). Since the number of data points in the present study are limited, the second region is poorly represented by our data and covers a very narrow range of pH (<0.5).

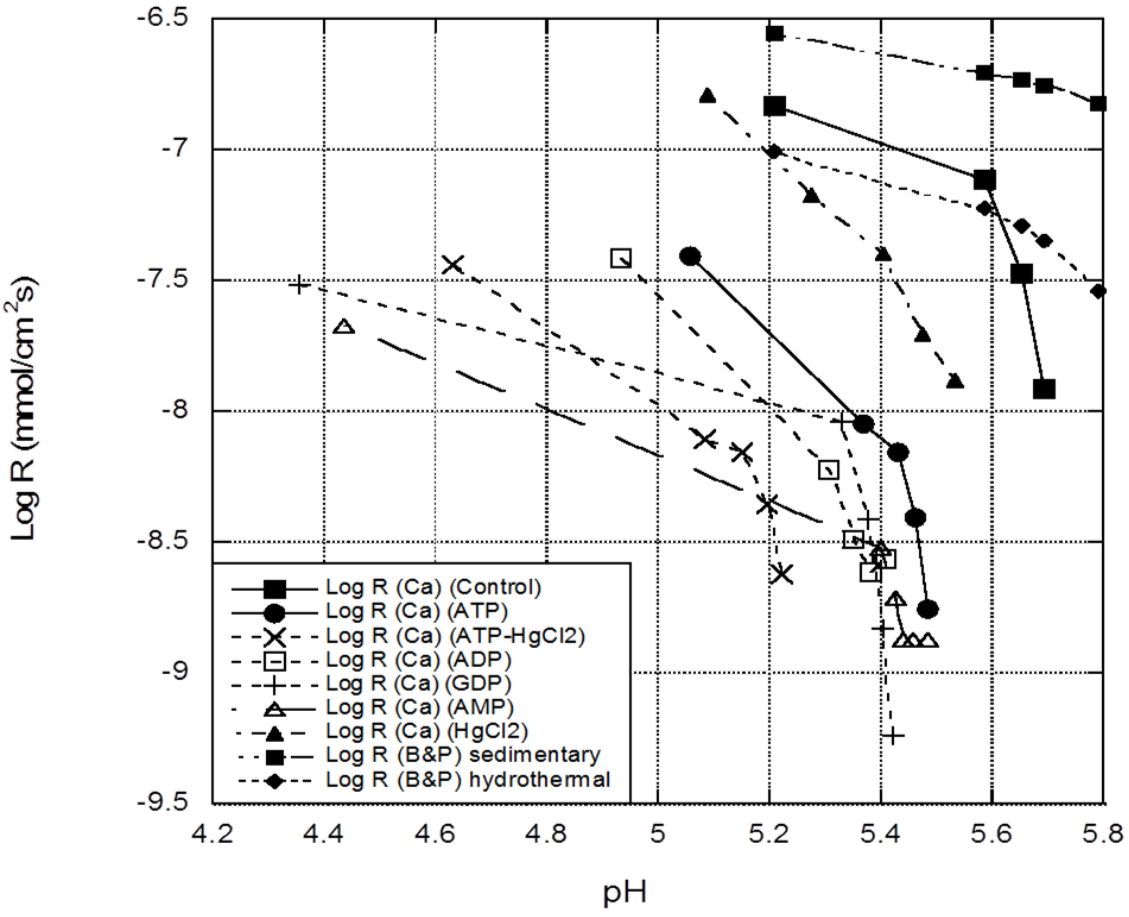

185

186 **Fig.2** Log (rate) of dolomite (as tracked by the release of Ca to the solution) vs. pH for dolomite
187 in the absence (control) and presence of selected nucleotides (Note that the reproducibility of rate
188 measurements, based on the results of replicate control experiments, was estimated at ≤4%). (The
189 B&P data are from Busenberg and Plummer (1982) and were acquired using sedimentary and
190 hydrothermal dolomite dissolved in distilled water at ambient temperature and at a pCO_2 ~1atm.)

191

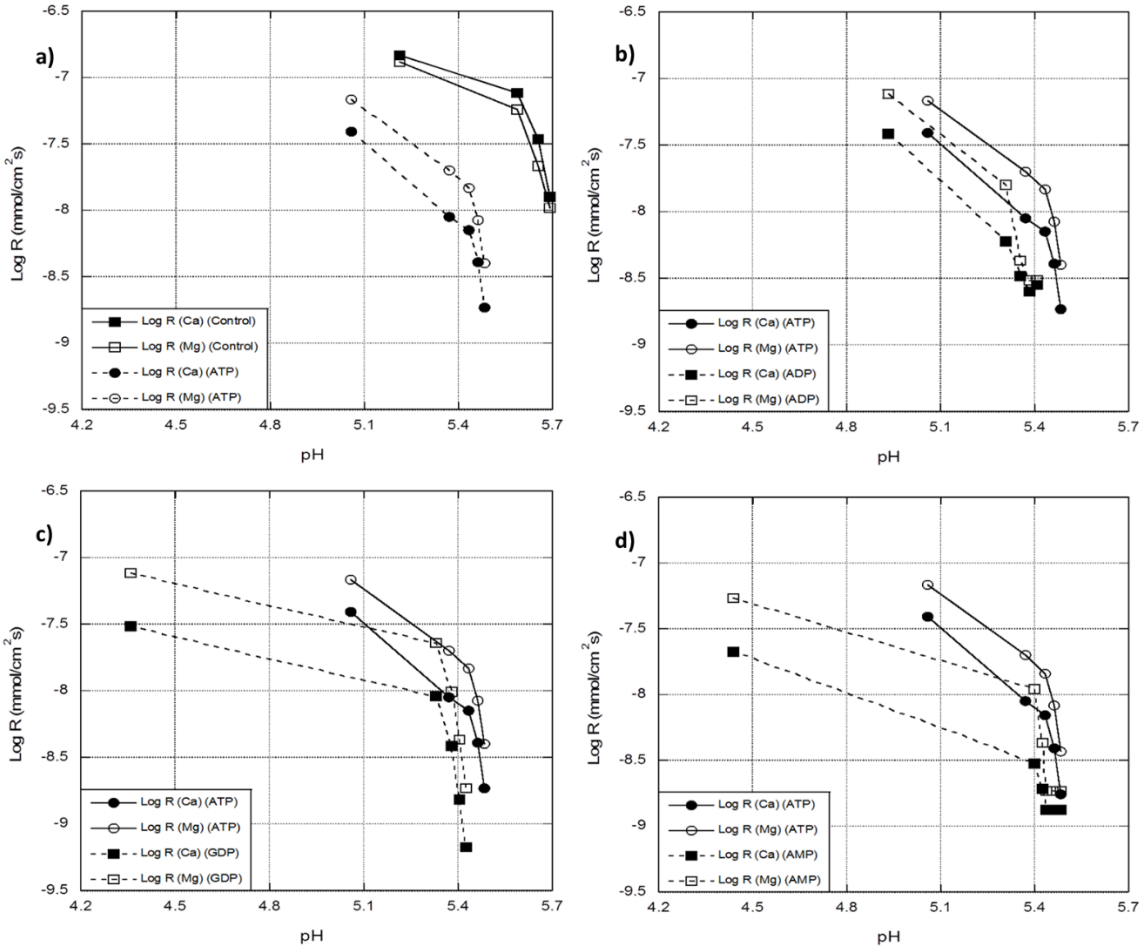

192

193 **Fig.3** Log (rate) of dolomite dissolution (as tracked by the release of Ca and Mg to the solution)
194 as a function of pH: a) Control vs. ATP, b) ATP vs ADP, c) ATP vs GDP and d) ATP vs AMP.
195 (Note that the reproducibility of rate measurements, based on the results of replicate control
196 experiments, was estimated at ≤4%.)

197

In Fig. 3, the dissolution rate of dolomite at various pHs in the presence and absence (control) of the selected nucleotides is presented in terms of the release rate of both Ca and Mg to the solutions. Our results indicate that the studied nucleotides not only inhibit the dissolution of dolomite, but also influence the stoichiometry of the dissolution reaction. Whereas the Mg:Ca ratio in the control experiment is nearly equal to the stoichiometry of the solid (Mg/Ca = 0.81 vs 0.76), it is much larger in the presence of the nucleotides (Mg/Ca = 1.9 to 2.7) (Table A-2). In other words, the dissolution of dolomite is highly incongruent in the presence of the nucleotides, with Mg being released to solution at a much faster rate than calcium. Our results contrast strongly with observations of Busenberg and Plummer (1982), Pokrovsky and Schott (2001), Zhang et al. (2007) and Urosevic et al. (2012) who reported that, , under acidic conditions (pH < 5) in deionized water, Ca dissolves faster than Mg and the surface of the dissolving dolomite becomes enriched with $MgCO_3$. To the best of our knowledge, the level of incongruency that we observed in the presence of the nucleotides has never been reported before, whether in the presence or absence of organic or inorganic additives (Pokrovsky and Schott, 2001; Thomas et al., 1993). The preferential release of Ca to the solution reported in previous studies of the dissolution of dolomite and other mixed cation minerals in water was explained by the lower hydration energy of Ca^{2+} relative to Mg^{2+} and the adsorption of Mg^{2+} at the mineral-water interface (Pokrovsky and Schott, 2001; Urosevic et al., 2012; Wang, 2012). The dissolution rates of dolomite, in the presence of ATP and a small amount of $HgCl_2$ ($5x10^{-5}$M, a strong bactericide), were also incongruent but slightly slower than those obtained in the absence of $HgCl_2$ (Fig. 4). Since the presence of $HgCl_2$, at an identical concentration, does not affect the stoichiometry but slightly inhibits the dolomite dissolution reaction in control experiments (no additives added) (Fig. 4), the observed rate inhibition and incongruency observed in the presence of the nucleotide upon the addition of $HgCl_2$ can be taken

as evidence that the influence of the nucleotide is not bacterially-mediated but a true abiotic response.

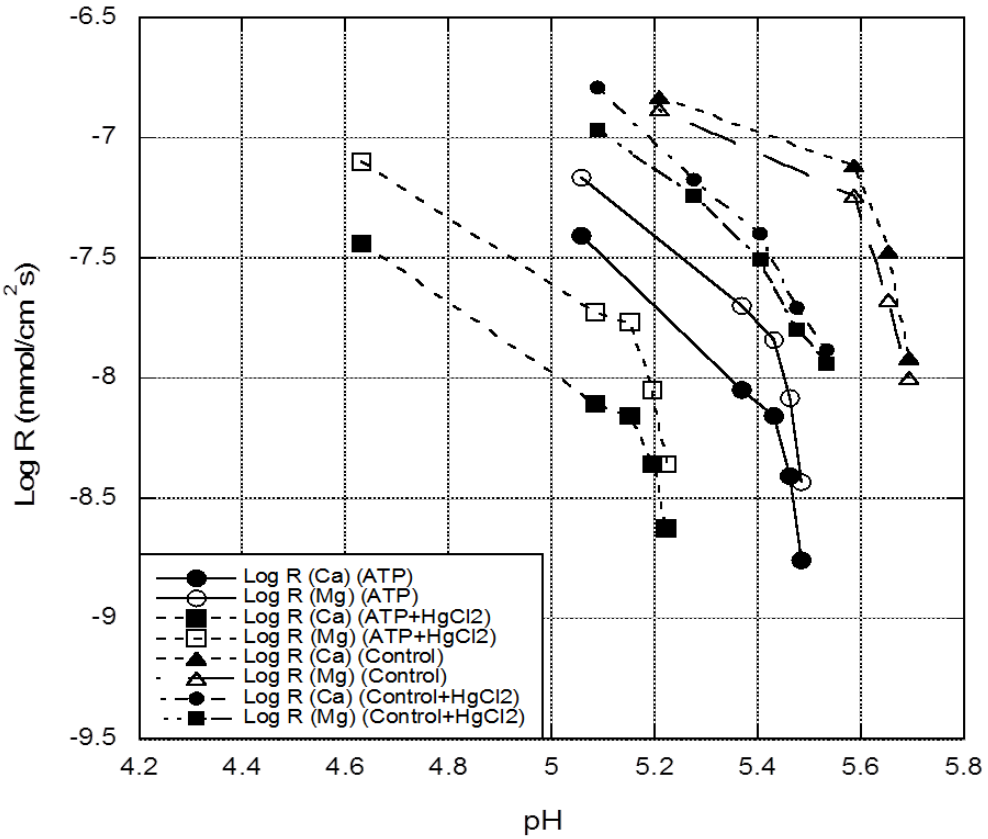

Fig.4 Log (rate) of dolomite dissolution (based on Ca and Mg release to the solution) as a function of pH: ATP vs. ATP-$HgCl_2$ and Control vs Control-$HgCl_2$. (Note that the reproducibility of rate measurements, based on the results of replicate control experiments, was estimated at ≤4%.)

3.2. Identification of the nucleotide structural component responsible for the incongruent dissolution behavior of dolomite

In order to identify which of the nucleotide's structural component (nucleoside, nitrogenous base, pentose sugar and phosphate) is responsible for the observed incongruent dolomite dissolution, we repeated the dissolution experiments in the presence of adenine, adenosine, guanine, guanosine and D-ribose as well as sodium monophosphate, diphosphate, triphosphate and hexametaphosphate salts. The results obtained in the presence of each nucleotide and their respective structural components are presented in Fig. 5, 6, 7 and 8. Among the components investigated, the phosphates, i.e. mono-, di- and tri-phosphates displayed similar behaviors to the nucleotides (ATP, ADP, GDP and AMP), whereas the other components (nucleoside, nitrogenous base and pentose sugar), like the control experiments, all lead to the congruent dissolution of dolomite, i.e., $Ca/Mg \approx 1$.

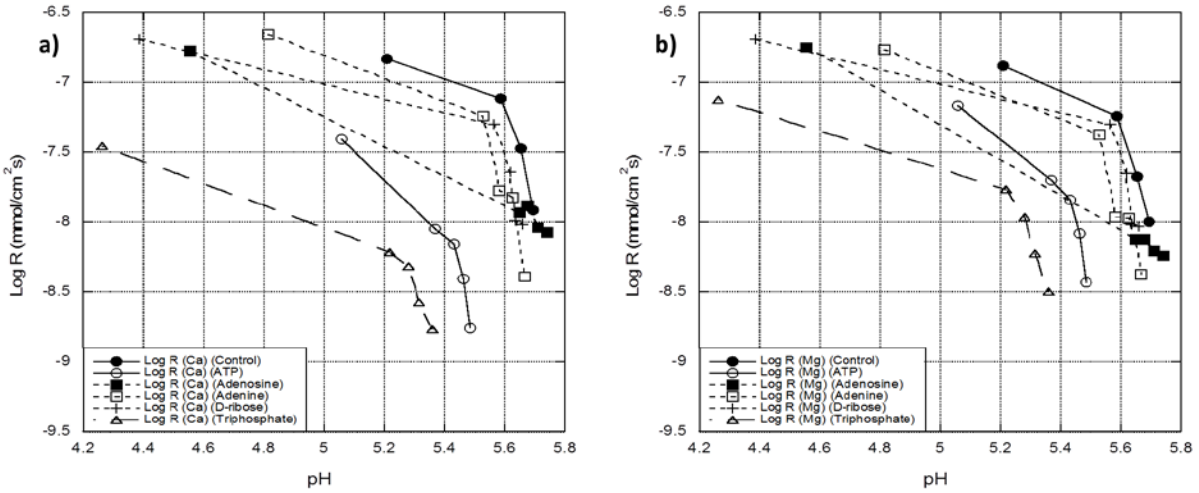

Fig.5 Dolomite dissolution rate (log) in terms of a) change in solution [Ca^{2+}] and b) [Mg^{2+}] as function of pH in the presence of 1mM ATP and its structural components: adenosine, adenine, D-ribose and triphosphate. (Note that the reproducibility of rate measurements, based on the results of replicate control experiments, was estimated at ≤4%.)

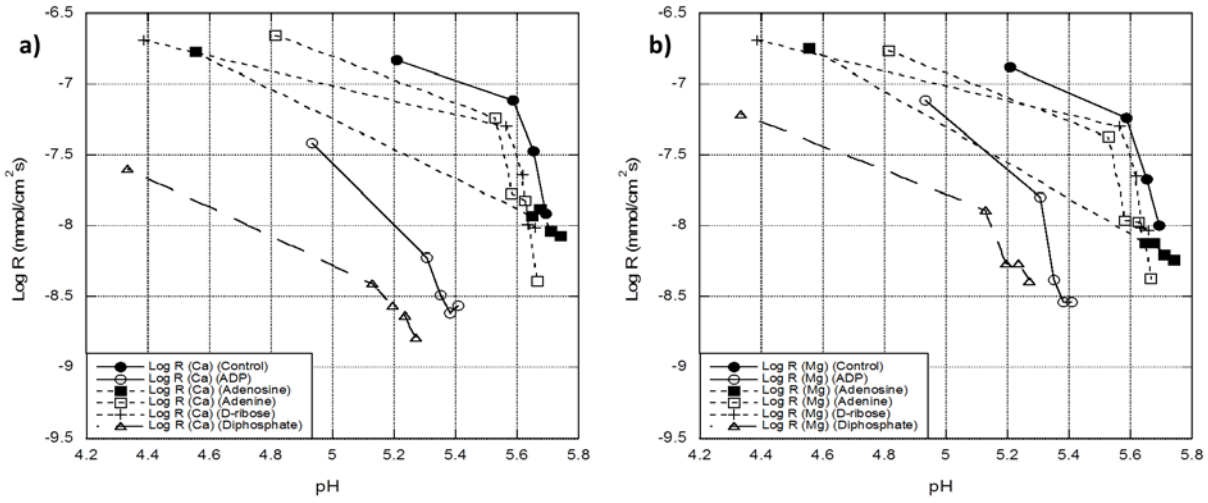

249

250 **Fig.6** Dolomite dissolution rate (log) in terms of a) change in solution [Ca^{2+}] and b) [Mg^{2+}] as
251 function of pH in the presence of 1mM ADP and its structural components: adenosine, adenine,
252 D-ribose and diphosphate. (Note that the reproducibility of rate measurements, based on the
253 results of replicate control experiments, was estimated at ≤4%.)

254

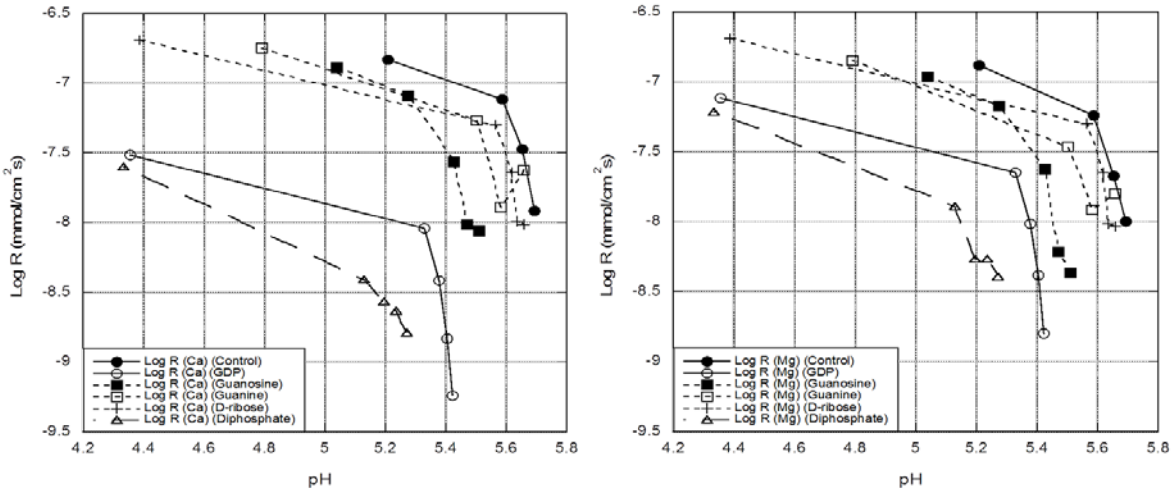

255

256 **Fig.7** Dolomite dissolution rate (log) in terms of a) change in solution [Ca^{2+}] and b) [Mg^{2+}] as
257 function of pH in the presence of 1mM GDP and its structural components: guanosine, guanine,
258 D-ribose and diphosphate. (Note that the reproducibility of rate measurements, based on the
259 results of replicate control experiments, was estimated at ≤4%.)

260

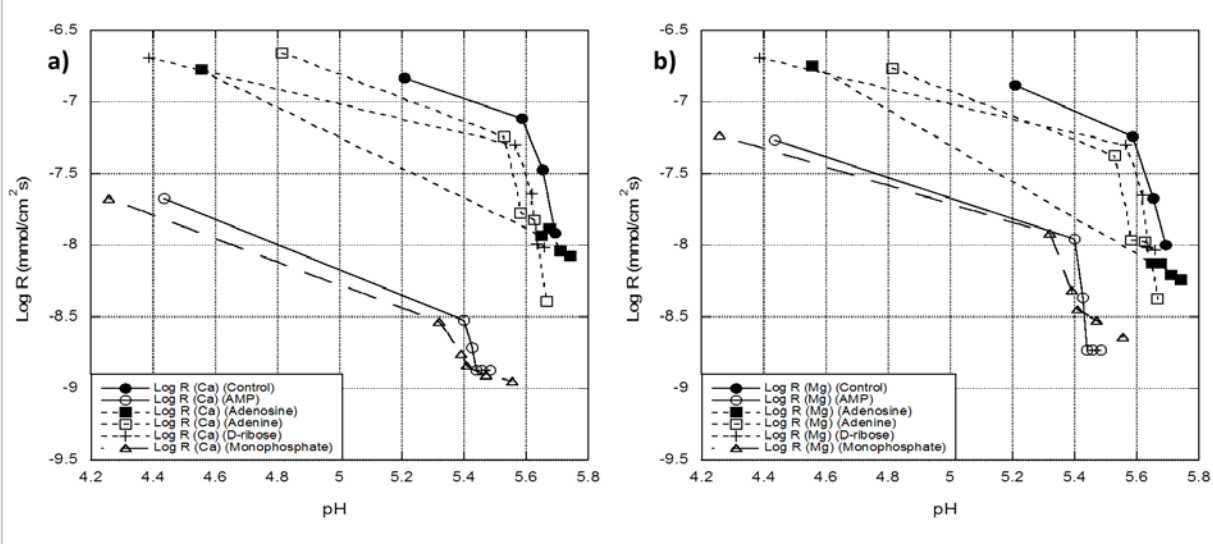

Fig.8 Dolomite dissolution rate (log) in terms of a) change in solution [Ca^{2+}] and b) [Mg^{2+}] as function of pH in the presence of 1mM AMP and its structural components: adenosine, adenine, D-ribose and monophosphate. (Note that the reproducibility of rate measurements, based on the results of replicate control experiments, was estimated at ≤4%.).

3.3. Influence of phosphate chain length on dolomite dissolution kinetics and stoichiometry

In order to quantify the extent of dolomite dissolution inhibition and the incongruency of the reaction by the phosphate moieties of the nucleotides, dolomite dissolution experiments were carried out in the presence of different phosphate salts (mono-, di-, tri- and hexametaphosphates). In Busenberg and Plummer (1982), dolomite dissolution rates are expressed as a function of the activity of H^+, H_2CO_3, H_2O and HCO_3^- and the rates slow as $aHCO_3^-$ increases in solution at a fixed pCO_2. In analogy to their study, we compare the effectiveness of the nucleotides and phosphate salts as inhibitors of dolomite dissolution at fixed HCO_3^- concentrations ($[HCO_3^-]$ (as opposed to activities, a thermodynamic construct inappropriate to express c kinetics). Note that we do not wish to imply a mechanistic role to the HCO_3^- ion in the dissolution reaction, it is simply used as a benchmark variable because rates vary almost linearly with its concentration,

The relative rates of dolomite dissolution with respect to the control experiment at identical $\log([HCO_3^-])$ in the presence of various nucleotides and phosphate salts are given in Fig. 9. The experimental results indicate that the degree of dissolution inhibition and incongruency is different for all tested phosphate salts. With the exception of monophosphate, dissolution inhibition increases as the phosphate chain becomes shorter, in the order AMP> ADP> ATP and diphosphate> triphosphate> monophosphate>hexametaphosphate, respectively. Given that the most powerful inhibiting species are believed to be the fully deprotonated phosphate moieties (Burton and Walter, 1990), the anomalous behavior of the monophosphate may reflect the fact that, under our experimental conditions and given their respective acidity constants (Table 2), the PO_4^{3-} concentration is smaller than that of triphosphate (TPP (5-)) and diphosphate (DPP (4-)) at the same total additive concentration (1mM).

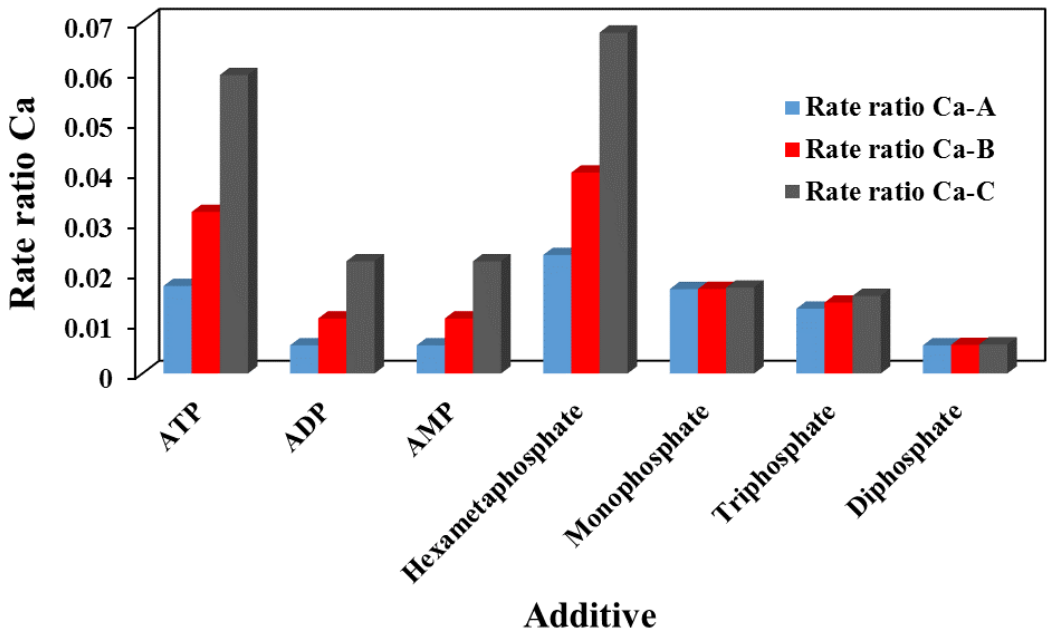

289

290 **Fig.9** Ratios of the dissolution rate of dolomite, as expressed by the release of Ca to solution, in
291 the presence of nucleotides and phosphate salts with respect to those measured in the control
292 experiment at three fixed log([HCO_3^-]) A) -2.00, B) -2.25 and C) -2.50. (Note that the ratios are
293 nearly the same if the rates are expressed in terms of the release of Mg to solution and [HCO_3^-]
294 values are calculated from the pH and pCO_2 of the individual experiments).

295

296 Earlier studies of dolomite dissolution (Busenberg and Plummer, 1982; Chou et al., 1989)
297 revealed that, in contrast to calcite (Alkattan et al., 1998; Pokrovsky et al., 2005), the kinetics of
298 dolomite dissolution is surface-reaction controlled even at low pH (i.e., <4). Nevertheless, Orton
299 and Unwin (1993) reported that, at low pH (3 to 4), the kinetics of dissolution is diffusion-
300 controlled, by providing evidence of mass-transport control on the dolomite dissolution rate.
301 Results of our control experiments at five different stirring rates (30 to 360 rpm) (Appendix, Fig.
302 A-1) reveal that the dissolution rates are congruent and do not vary systematically with stirring
303 rate and are therefore deemed surface reaction-controlled. Our experimental observation at the
304 lowest stirring rate (30 rpm), with the mineral grains sitting nearly undisturbed at the bottom of
305 reaction vessel, clearly support our conclusion whereas the odd data obtained at the highest stirring
306 rate (360 rpm) are most likely an experimental artifact that results from the collision between the
307 mineral grains. In summary, whereas the investigated nucleotides and most of their structural
308 components inhibited the dolomite dissolution rate, a greater inhibition and incongruent
309 dissolution were observed when the investigated compounds contained phosphate moieties.

310 Several studies have reported the inhibitory effect of phosphate (Alkattan et al., 2002; Dove
311 and Hochella, 1993; Klasa et al., 2013; Lin and Singer, 2005; Morse, 1974; Mucci, 1986; Sjöberg,
312 1978; Sulu-Gambari, 2011; Walter and Burton, 1986) and nucleotides (Meyer, 1984) on calcite
313 dissolution and growth, but the influence of nucleotides and phosphate salts on dolomite
314 dissolution kinetics has not been investigated before. Phosphate inhibits the dissolution and growth
315 of calcite by adsorbing at high energy sites (kink, step, edge and hole) on the mineral surface
316 (Berner and Morse, 1974; Giannimaras and Koutsoukos, 1987; Meyer, 1984; Mucci, 1986; Walter
317 and Burton, 1986) and leads to variations in etch-pit spreading and step-retreat rates (Ruiz-Agudo
318 and Putnis, 2012). The inhibition is believed to be caused by the temporary pinning of phosphate

at active sites and the consequent impediment of anion attachment (growth) or cation detachment (dissolution) from neighboring sites (Berner and Morse, 1974; Dove and Hochella, 1993). Alternatively, our observations could be explained by the concomitant release of calcium and magnesium from the dolomite, followed by the precipitation of their corresponding phosphate salts on the mineral surface (Klasa et al., 2013; Xu et al., 2014a; Xu et al., 2014b; Yuan et al., 2015) and further dissolution inhibition. In other words, the incongruent dissolution of dolomite in the presence of phosphate-containing compounds may reflect the preferential adsorption of phosphate species such as $CaHPO_4^0$ (Lin and Singer, 2006) and precipitation of a phosphate phase on the mineral surface. Like Xu et al (2014a), we do not exclude the possible adsorption of Mg and formation of Mg-phosphate phases.

The adsorption of phosphate-bearing compounds on calcite has been investigated in various contexts such as its influence on the mineral dissolution kinetics (Alkattan et al., 2002; Klasa et al., 2013) and growth (Dove and Hochella, 1993; Giannimaras and Koutsoukos, 1987; Lin and Singer, 2005; Lin and Singer, 2006; Plant and House, 2002), surface-complexation model development (Sø et al., 2011; Xu et al., 2014a), the use of calcite as a phosphate adsorbing substrate (Freeman and Rowell, 1981; Karageorgiou et al., 2007; Millero et al., 2001; Prochaska and Zouboulis, 2006; Sawada et al., 2003; Sø et al., 2011; Suzuki et al., 1986; Wang et al., 2012) and phosphate mineral nucleation and replacement (Rokidi et al., 2011;Wang et al., 2012). Most of these studies were conducted using monophosphate, with a limited number of investigations of pyrophosphate (Lin and Singer, 2005), triphosphate (Sawada et al., 2003), polymetaphosphates (Lin and Singer, 2005) and nucleotides (Cleaves et al., 2011). To the best of our knowledge, the influence of phosphate on dolomite dissolution and growth kinetics has not been investigated, but a number of studies of its adsorption to natural as well as calcinated dolomite (Hanna et al., 2008;

Karaca et al., 2004; Karaca et al., 2006; Mangwandi et al., 2014; Nugroho et al., 2014; Roques et al., 1991; Xu et al., 2014a; Yuan et al., 2015) and the pseudomorphic transformation of dolomite to a phosphate mineral (Schultheiss et al., 2013) can be found in the literature. In most of these studies, the authors state that the interaction of mineral constituent cations in solution or at the mineral surface with phosphate commonly leads to the formation of various calcium and magnesium phosphate phases such as amorphous calcium phosphate (ACP) (Dove and Hochella, 1993; Giannimaras and Koutsoukos, 1987; Millero et al., 2001; Roques et al., 1991; Wang et al., 2012; Xu et al., 2014a; Xu et al., 2014b), hydroxyapatite (HAP) (Klasa et al., 2013; Yuan et al., 2015; Schultheiss et al., 2013), di-calcium phosphate (DCP) (Freeman and Rowell, 1981), di-basic calcium phosphate di-hydrate (DCPD) (Xu et al., 2014b), tri-calcium phosphate (TCP) (Plant and House, 2002; Sawada et al., 2003), octa-calcium phosphate (OCP) (Freeman and Rowell, 1981; Klasa et al., 2013; Plant and House, 2002; Sawada et al., 2003), newberyite ($MgHPO_4.3H_2O$) (Xu et al., 2014a) and whitlockite ($Ca_9Mg(PO_4)_6(PO_3OH)$) (Schultheiss et al., 2013). As discussed previously, the metal phosphate phases can either form following the adsorption of phosphate at the mineral surface and the formation of surface complexes (Giannimaras and Koutsoukos, 1987; Sø et al., 2011) or following dolomite dissolution and release of calcium to the solution, its adsorption and precipitation of a Ca-phosphate phase on the surface (Klasa et al., 2013; Yuan et al., 2015). There have also been reports of the hydrothermal mineral replacement of calcite and aragonite by calcium phosphate phases (apatite, HAP and second phosphate phase β-TCP) (Jonas et al., 2014; Lemos et al., 2006; Yoshimura et al., 2004). Under acidic or circum-neutral conditions ($pH \leq 7$), the following surface complexes: $>CaH_2PO_4^+$, $>CaHPO_4^0$ and $>MgHPO_4Ca^+$ are thought to dominate and serve as precursors of a Ca-phosphate phase (Giannimaras and Koutsoukos, 1987; Lin and Singer, 2006; Hanna et al., 2008; Xu et al., 2014a). At $pH \geq 8$, $>CaPO_4Ca^0$ and

365 >$MgHPO_4Ca^+$ would prevail and lead to the formation of both Ca- and Mg-phosphates (e.g.,
366 newberyite; Xu et al., 2014a).

367 Given that this study was conducted at a high pCO_2 (~1 atm) and weak acidic conditions
368 (pH ~4-6), and since the Mg:Ca ratio in solution is significantly larger than the mineral
369 stoichiometry, the observed inhibition and reaction incongruency is best explained by the
370 adsorption of phosphate (or $CaHPO_4^0$, as proposed by Lin and Singer (2006)) at $CaCO_3$ sites
371 through pinning of active dissolution sites (steps) followed by the growth of a Ca-phosphate phase
372 on the dolomite surface, by the formation of a (Ca, Mg)-phosphate overgrowth and/or the surface
373 adsorption of Mg ions (Schultheiss et al., 2013). Calculations of the saturation indices (SI = log
374 (Ω) = log (IAP/K^o_{sp})) of the experimental solutions with respect to different Me (Ca, Mg)-
375 phosphate phases (ACP, HAP, TCP, OCP, DCPD and newberyite) throughout the dolomite
376 dissolution reaction (Table A-3), reveal that the solutions were undersaturated with respect to these
377 minerals at all times. SEM micrographs (FEI Quanta 450 Environmental Scanning Electron
378 Microscope (FE-ESEM)) of the fresh ground dolomite (starting material) and reacted solids
379 recovered (washed with DI water and air dried) from the control, monophosphate and AMP
380 experiments are shown in Fig. 10 a, b, c and d, respectively. The samples were mounted on
381 aluminum stubs, sputter-coated with platinum and examined by scanning electron microscopy at
382 an accelerating voltage of 10KV. Whereas the surface of the first two shows well defined steps
383 and is devoid of fine particules, the solids reacted in the presence of monophosphate and AMP
384 display irregular and corroded surfaces and the presence (a frosting) of very fine overgrowths
385 concentrated along step edges and on flat surfaces. Following the complete dissolution of aliquots
386 of the fresh dolomite and the reacted solids (washed in DI water and air dried) from the control
387 and monophosphate experiments in a 5N HCl solution, the phosphate concentration of the

388 solutions was measured spectrophotometrically (HP-8453A UV-Visible diode-array
389 spectrophotometer) using the phosphomolybdate method developed by Murphy and Riley (1962)
390 and described in Grasshoff et al. (1999). The absorbance of the phosphomolybdate reaction
391 product was measured at 880 nm in a 1-cm quartz cell. Based on the results of our analyses, the
392 phosphate concentration on the solids reacted in the presence of monophosphate was 280 µmol/g
393 or 1.8 µmol/cm^2, whereas it was barely detectable (detection limit was 0.5 µmol/g or 0.003
394 µmol/cm^2) in the others samples. These results and the SEM photomicrographs confirm that a
395 phosphate phase was precipitated on the mineral surface. The preferential precipitation of a Ca-
396 phosphate, leading to the observed incongruent dissolution, is likely a consequence of the
397 differential stability of the surface complexes and the solubility product of the calcium and
398 magnesium phosphate salts (Table 3). The K_{sp} of common calcium phosphates vary between $2x10^{-33}$ (apatite) and $1x10^{-36}$ (hydroxyapatite), compared to magnesium phosphate $1.04x10^{-24}$
400 ($Mg_2(PO)_3$) and $1.67x10^{-6}$ (newberyite) at 25°C (Averill, 2012; Le Rouzic, 2013; Verbeeck et al.,
401 1984; Xu et al., 2014b). Whereas, under our experimental conditions, $H_2PO_4^-$, HPO_4^{2-} and
402 $CaHPO_4^0$ dominate in solution and PO_4^{3-} is negligible (<0.05%), Xu et al. (2014a) estimates that,
403 between pH 5.5 and 6.5, $>CaH_2PO_4^+$, $>CaHPO_4^0$ and $>MgHPO_4Ca^+$ are the dominant species on
404 the dolomite surface at total phosphate concentrations > 0.1mM. As mentioned above, fully
405 deprotonated phosphate (PO_4^{3-}) accounts for less than 0.05 % of total phosphate in solution, but it
406 is expected that its adsorption will lead to a re-equilibration of the dissolved phosphate species (Le
407 Chatelier's principle). Hence, over the course of the experiment, a potentially significant amount
408 of PO_4^{3-} may adsorb onto the dolomite surface. It is also interesting to note that the presence of
409 Mg in calcite and dolomite enhances phosphate adsorption to their surfaces and may promote the

410 precipitation of a Ca-phosphate phase on the mineral surface (Millero et al., 2001; Xu et al.,
411 2014a).
412

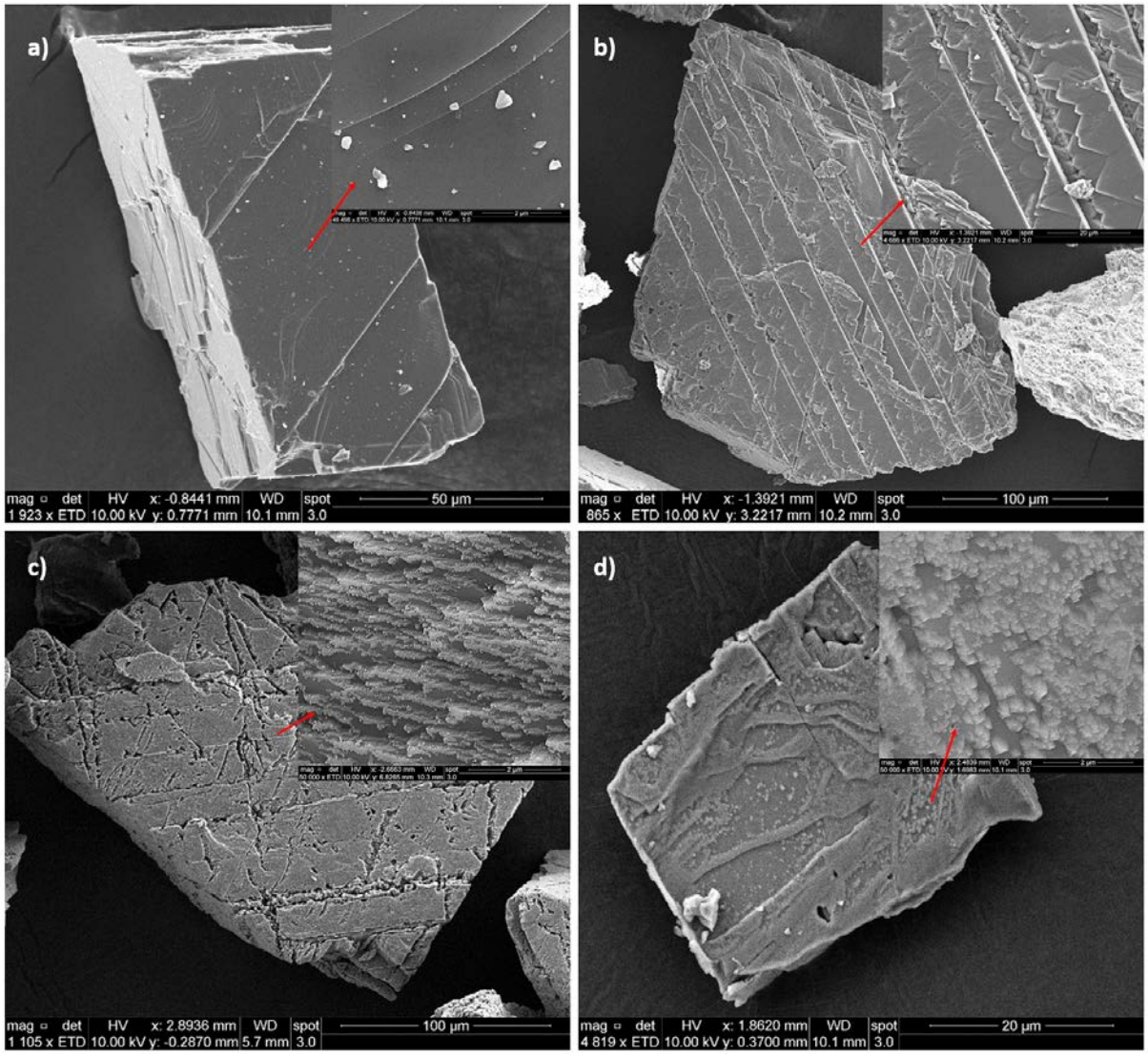

413

414 **Fig.10** SEM micrographs of a) fresh, ground dolomite (starting material) and recovered, reacted

415 solids of b) control, c) monophosphate and d) AMP experiments.

416

4. Conclusion

Dolomite dissolution rate and stoichiometry were determined at 25°C and 1 atm pCO_2 to simulate conditions that may be encountered during geological CO_2 sequestration in carbonate aquifers. The study was conducted in the absence (control) and presence (1mM) of the nucleotides (ATP, ADP, GDP and AMP) and their structural components (adenine, guanine, D-ribose, adenosine and guanosine), including inorganic phosphate salts (mono-, di-, tri- and hexametaphosphates), that are likely present in deep aquifers at low concentrations (1-10mM). With the exception of adenine and D-ribose, the presence of all nucleotides, their structural components, including all phosphate salts inhibited the dolomite dissolution rate relative to the control experiment. The presence of nucleotides and phosphate salts not only inhibited the dolomite dissolution but also lead to an incongruent reaction, yielding a resultant solution with a Mg:Ca molar ratio ≥ 2. With the exception of monophosphate, the inhibition was found to increase as the length of the chained phosphate nucleotides and inorganic polyphosphates decreased. Under our experimental conditions, the dissolution of dolomite in the presence of nucleotides and phosphate is accompanied by the nucleation of a solid phosphate phase on the dolomite surface, as resolved by SEM and confirmed by phosphate analysis of the dissolved reacted solids. The surface precipitate is likely a Ca-rich phosphate phase, accounting for the observed incongruent dissolution. Since the reacting solutions were undersaturated with respect to common Ca and Mg-phosphate phases throughout the dissolution experiments, adsorption of phosphate followed by the development of a Me (Ca, Mg)-phosphate phase through surface complexation is thought to account for the observed incongruency. Whereas the formation of a carbonate hydroxyapatite has been documented by atomic force microscopy (AFM) on the surface of dissolving calcite in the presence of phosphate salts (Kamiya et al., 2004; Klasa et al., 2013), a similar study of the dolomite

surface has not yet been conducted to confirm the nature of the precipitate at low temperatures, but whilockite was shown to form under hydrothermal conditions (Schultheiss et al., 2013).

The present study provides insights on how dolomite behaves upon dissolution in the presence of the studied additives in low ionic strength solutions. A more pertinent study, in the context of CO_2 sequestration in deep aquifers (subsurface environments, high ionic strengths to brine like conditions), would require an investigation of the effect of ionic strength on the dolomite dissolution rate in the absence and presence of these additives (Jordan et al., 2007; Oelkers et al., 2011; Pokrovsky and Schott, 2001; Pokrovsky et al., 2005; Pokrovsky et al., 2009a; Pokrovsky et al., 2009b).

Acknowledgements

This study was funded by grants from the Carbon Management Canada Networks of Centers of Excellence (project ID C-3-093) and the Natural Sciences and Engineering Council of Canada Discovery program to A.M. Dr. Takeshi Arakaki's visit and sabbatical leave at McGill University was sponsored by the Okinawa International University.

References

Alberty, R.A., Smith, R.M., Bock, R.M., 1951. The apparent ionization constants of the adenosinephosphates and related compounds. Journal of Biological Chemistry. 193(1): 425-434.

Alkattan, M., Oelkers, E.H., Dandurand, J.-L., Schott, J., 1998. An experimental study of calcite and limestone dissolution rates as a function of pH from -1 to 3 and temperature from 25 to 80^{0}C. Chemical Geology. 151(1): 199-214.

Alkattan, M., Oelkers, E.H., Dandurand, J.-L., Schott, J., 2002. An experimental study of calcite dissolution rates at acidic conditions and 25^{0}C in the presence of $NaPO_3$ and $MgCl_2$. Chemical Geology. 190(1): 291-302.

André, L., Audigane, P., Azaroual, M., Menjoz, A., 2007. Numerical modeling of fluid–rock chemical interactions at the supercritical CO_2–liquid interface during CO_2 injection into a carbonate reservoir, the Dogger aquifer (Paris Basin, France). Energy Conversion and Management. 48(6): 1782-1797.

André, L., Azaroual, M., Menjoz, A., 2010. Numerical simulations of the thermal impact of supercritical CO_2 injection on chemical reactivity in a carbonate saline reservoir. Transport in Porous Media. 82(1): 247-274.

Arvidson, R.S., Mackenzie, F.T., 1999. The dolomite problem; control of precipitation kinetics by temperature and saturation state. American Journal of Science. 299(4): 257-288.

Averill, B.A., 2012. Principles of General Chemistry, New England, pp. 3023. http://2012books.lardbucket.org/books/principles-of-general-chemistry-v1.0/

Bachu, S., 2003. Screening and ranking of sedimentary basins for sequestration of CO_2 in geological media in response to climate change. Environmental Geology. 44(3): 277-289.

Bachu, S., Adams, J.J., 2003. Sequestration of CO_2 in geological media in response to climate change: capacity of deep saline aquifers to sequester CO_2 in solution. Energy Conversion and Management. 44(20): 3151-3175.

Bachu, S., Stewart, S., 2002. Geological sequestration of anthropogenic carbon dioxide in the Western Canada sedimentary basin: suitability analysis. Journal of Canadian Petroleum Technology. 41(02): 32-40.

Berner, R.A., Morse, J.W., 1974. Dissolution kinetics of calcium carbonate in sea water; IV, Theory of calcite dissolution. American Journal of Science. 274(2): 108-134.

Bulleid, N., 1978. An improved method for the extraction of adenosine triphosphate from marine sediment and seawater. Limnology and Oceanography. 23(1): 174-178.

Burton, E.A., Walter, L.M., 1990. The role of pH in phosphate inhibition of calcite and aragonite precipitation rates in seawater. Geochimica et Cosmochimica Acta. 54(3): 797-808.

Busenberg, E., Plummer, L.N., 1982. The kinetics of dissolution of dolomite in CO_2-H_2O systems at 1.5 to 65^{0}C and 0 to 1 atm pCO_2. American Journal of Science. 282(1): 45-78.

Chai, L., Navrotsky, A., Reeder, R., 1995. Energetics of calcium-rich dolomite. Geochimica et Cosmochimica Acta. 59(5): 939-944.

Chou, L., Garrels, R.M., Wollast, R., 1989. Comparative study of the kinetics and mechanisms of dissolution of carbonate minerals. Chemical Geology. 78(3): 269-282.

Cleaves, H.J., Crapster-Pregont, E., Jonsson, C.M., Jonsson, C.L., Sverjensky, D.A., Hazen, R.A., 2011. The adsorption of short single-stranded DNA oligomers to mineral surfaces. Chemosphere. 83(11): 1560-1567.

Creaney, S., Allan, J., 1990. Hydrocarbon generation and migration in the Western Canada Sedimentary Basin. Geological Society, London, Special Publications. 50(1): 189-202.

Dai Lam, T., Hoang, V.D., Le Ngoc Lien, N.N.T., Dien, P.G., 2006. Synthesis and characterization of chitosan nanoparticles used as drug carrier. Journal of Chemistry. 44(1): 105-109.

Dawson, R.M.C., Elliott, D.C., Elliott, W.H., Jones, K.M., 1989. Data for Biochemical Research. Clarendon Press, Oxford, UK.

Dhami, N.K., Reddy, M.S., Mukherjee, A., 2013. Biomineralization of calcium carbonates and their engineered applications: a review. Frontiers in Microbiology. 4: 314.

Dove, P.M., Hochella, M.F., 1993. Calcite precipitation mechanisms and inhibition by orthophosphate: In situ observations by Scanning Force Microscopy. Geochimica et Cosmochimica Acta. 57(3): 705-714.

Fowler, M.G., Stasiuk, L.D., Hearn, M., Obermajer, M., 2001. Devonian hydrocarbon source rocks and their derived oils in the Western Canada Sedimentary Basin. Bulletin of Canadian Petroleum Geology. 49(1): 117-148.

Freeman, J., Rowell, D., 1981. The adsorption and precipitation of phosphate onto calcite. Journal of Soil Science. 32(1): 75-84.

Garcia, M., Dávila, G., Offeddu, F., Soler, J.M., Cama, J., 2011. Reactions during CO_2 geological sequestration: Dissolution of calcite and dolomite coupled to gypsum precipitation. Rev. Soc. Esp. Mineral. 2: 93-94.

Gautelier, M., Oelkers, E.H., Schott, J., 1999. An experimental study of dolomite dissolution rates as a function of pH from− 0.5 to 5 and temperature from 25 to 80°C. Chemical Geology. 157(1–2): 13-26.

Gautelier, M., Schott, J., Oelkers, E.H., 2007. An experimental study of dolomite dissolution rates at 80°C as a function of chemical affinity and solution composition. Chemical Geology. 242(3–4): 509-517.

Giannimaras, E.K., Koutsoukos, P.G., 1987. The crystallization of calcite in the presence of orthophosphate. Journal of Colloid and Interface Science. 116(2): 423-430.

Grasshoff, K., Kremling, K., Ehrhardt, M., 2009. Methods of Seawater Analysis. John Wiley & Sons. New York, NY.

Gray, C.J., Engel, A.S., 2013. Microbial diversity and impact on carbonate geochemistry across a changing geochemical gradient in a karst aquifer. ISME J. 7(2): 325-337.

Halbertsma, H., 1994. Devonian Wabamun group of the Western Canada Sedimentary Basin. Geological Atlas of the Western Canada Sedimentary Basin. 4: 203-220.

Hamilton, W., Olson, R., 1990. Mineral Resources of the Western Canada Sedimentary Basin [Abstract]. Bulletin of Canadian Petroleum Geology. 38(1): 165-165.

Hanna, A., Sherief, M., Abo Elenin, R., 2008. Phosphate removal from wastewater by calcite and dolomite ores. Phosphorus Research Bulletin. 22: 7-12.

Hao, Y., Smith, M., Sholokhova, Y., Carroll, S., 2013. CO_2-induced dissolution of low permeability carbonates. Part II: Numerical modeling of experiments. Advances in Water Resources. 62: 388-408.

Hay, P., 1994. Oil and gas resources of the Western Canada Sedimentary Basin. GD Mossop and I. Shetsen, comps., Geological atlas of the Western Canada sedimentary basin. Canadian Society of Petroleum Geologists and Alberta Research Council, Calgary: 469-470.

Herman, J.S., 1982. The dissolution kinetics of calcite, dolomite, and dolomitic rocks in the CO_2-water system. Unpublished PhD thesis, Pennsylvania State University. 219p.

Herman, J.S., White, W.B., 1985. Dissolution kinetics of dolomite: effects of lithology and fluid flow velocity. Geochimica et Cosmochimica Acta. 49(10): 2017-2026.

Holm Hansen, O., Booth, C.R., 1966. The measurement of adenosine triphosphate in the ocean and its ecological significance. Limnology and Oceanography. 11(4): 510-519.

Jonas, L., John, T., King, H.E., Geisler, T., Putnis, A., 2014. The role of grain boundaries and transient porosity in rocks as fluid pathways for reaction front propagation. Earth and Planetary Science Letters. 386: 64-74.

Jordan, G., Pokrovsky, O.S., Guichet, X., Schmahl, W.W., 2007. Organic and inorganic ligand effects on magnesite dissolution at 100^0C and pH= 5 to 10. Chemical Geology. 242(3): 484-496.

Kamiya, M., Hatta, J., Shimada, E., Ikuma, Y., Yoshimura, M., Monma, H., 2004. AFM analysis of initial stage of reaction between calcite and phosphate. Materials Science and Engineering: B. 111(2): 226-231.

Karaca, S., Gürses, A., Ejder, M., Açıkyıldız, M., 2004. Kinetic modeling of liquid-phase adsorption of phosphate on dolomite. Journal of Colloid and Interface Science. 277(2): 257-263.

Karaca, S., Gürses, A., Ejder, M., Açıkyıldız, M., 2006. Adsorptive removal of phosphate from aqueous solutions using raw and calcinated dolomite. Journal of Hazardous Materials. 128(2): 273-279.

Karageorgiou, K., Paschalis, M., Anastassakis, G.N., 2007. Removal of phosphate species from solution by adsorption onto calcite used as natural adsorbent. Journal of Hazardous Materials. 139(3): 447-452.

Karl, D., Craven, D., 1980. Effects of alkaline phosphatase activity on nucleotide measurements in aquatic microbial communities. Applied and Environmental Microbiology. 40(3): 549-561.

Klasa, J., Ruiz-Agudo, E., Wang, L., Putnis, C., Valsami-Jones, E., Menneken, M., Putnis, A., 2013. An atomic force microscopy study of the dissolution of calcite in the presence of phosphate ions. Geochimica et Cosmochimica Acta. 117: 115-128.

Le Rouzic, M., 2013. Conditions de formation de la k-struvite dans les ciments phosphomagnésiens, 31ème rencontres Universitaire de l'AUGC, pp. 8p.

Lemos, A., Rocha, J., Quaresma, S., Kannan, S., Oktar, F., Agathopoulos, S., Ferreira, J., 2006. Hydroxyapatite nano-powders produced hydrothermally from nacreous material. Journal of the European Ceramic Society. 26(16): 3639-3646.

Lin, Y.-P., Singer, P.C., 2005. Inhibition of calcite crystal growth by polyphosphates. Water Research. 39(19): 4835-4843.

Lin, Y.-P., Singer, P.C., 2006. Inhibition of calcite precipitation by orthophosphate: speciation and thermodynamic considerations. Geochimica et Cosmochimica Acta. 70(10): 2530-2539.

Luhmann, A.J., Kong, X.-Z., Tutolo, B.M., Garapati, N., Bagley, B.C., Saar, M.O., Seyfried Jr, W.E., 2014. Experimental dissolution of dolomite by CO_2-charged brine at 100°C and 150 bar: Evolution of porosity, permeability, and reactive surface area. Chemical Geology. 380: 145-160.

Luquot, L., Gouze, P., 2009. Experimental determination of porosity and permeability changes induced by injection of CO_2 into carbonate rocks. Chemical Geology. 265(1): 148-159.

Lüttge, A., Winkler, U., Lasaga A.C. (2003) Interferometric study of the dolomite dissolution: A new conceptual model for mineral dissolution. Geochimica et Cosmochimica Acta.67: 1099-1116.Machel, H.G., Krouse, H.R., Sassen, R., 1995. Products and distinguishing criteria of bacterial and thermochemical sulfate reduction. Applied Geochemistry. 10(4): 373-389.

Mangwandi, C., Albadarin, A.B., Glocheux, Y., Walker, G.M., 2014. Removal of ortho-phosphate from aqueous solution by adsorption onto dolomite. Journal of Environmental Chemical Engineering. 2(2): 1123-1130.

McKenzie, J.A., Vasconcelos, C., 2009. Dolomite Mountains and the origin of the dolomite rock of which they mainly consist: historical developments and new perspectives. Sedimentology. 56(1): 205-219.

Meyer, H., 1984. The influence of impurities on the growth rate of calcite. Journal of Crystal Growth. 66(3): 639-646.

Millero, F., Huang, F., Zhu, X., Liu, X., Zhang, J.-Z., 2001. Adsorption and desorption of phosphate on calcite and aragonite in seawater. Aquatic Geochemistry. 7(1): 33-56.

Mohamed, I.M., He, J., Nasr-El-Din, H.A., 2011. Carbon dioxide sequestration in dolomite rock, International Petroleum Technology Conference. International Petroleum Technology Conference, Bangkok, Thailand.

Morse, J.W., 1974. Dissolution kinetics of calcium carbonate in sea water; V, Effects of natural inhibitors and the position of the chemical lysocline. American Journal of Science. 274(6): 638-647.

Morse, J.W., Arvidson, R.S., 2002. The dissolution kinetics of major sedimentary carbonate minerals. Earth-Science Reviews. 58(1–2): 51-84.

Morse, J.W., Arvidson, R.S., Lüttge, A., 2007. Calcium carbonate formation and dissolution. Chemical Reviews. 107(2): 342-381.

Mucci, A., 1986. Growth kinetics and composition of magnesian calcite overgrowths precipitated from seawater: Quantitative influence of orthophosphate ions. Geochimica et Cosmochimica Acta. 50(10): 2255-2265.

Murphy, J., Riley, J.P., 1962. A modified single solution method for the determination of phosphate in natural waters. Analytica Chimica Acta. 27: 31-36.

Nugroho, F.L., Mulyatna, L., Situmeang, A.D.W., 2014. Removal of phosphate from synthetic aqueous solution by adsorption with dolomite from Padalarang. Journal of Engineering and Technological Sciences. 46(4): 410-419.

Oelkers, E.H., Golubev, S.V., Pokrovsky, O.S., Bénézeth, P., 2011. Do organic ligands affect calcite dissolution rates?. Geochimica et Cosmochimica Acta. 75(7): 1799-1813.

Oelkers, E.H., Schott, J., 2005. Geochemical aspects of CO_2 sequestration. Chemical Geology. 217(3–4): 183-186.

Oomori, T., Kitano, Y., 1991. Effect of phosphorous-containing compounds on polymorphic formation of calcium carbonate. In: Suga, S., Nakahara, H. (Eds.), Mechanisms and Phylogeny of Mineralization in Biological Systems. Springer-Verlag, Tokyo, Japan, pp. 501-505.

Orton, R., Unwin, P.R., 1993. Dolomite dissolution kinetics at low pH: a channel-flow study. J. Chem. Soc., Faraday Trans. 89(21): 3947-3954.

Parkhurst, D., Appelo, C., 2011. PHREEQC version 3–A computer program for speciation, batch-reaction, one-dimensional transport, and inverse geochemical calculations. U.S. Geological Survey Techniques and Methods, book 6, chap. A43, 497 p., available only at http://pubs.usgs.gov/tm/06/a43/.

Paul, V.G., 2014. Biomineralization of carbonates in modern microbial sediments and its implications for CO_2 sequestration, Missouri University of Science and Technology, 257 pp.

Perrin, D.D., 1982. Ionisation constants of inorganic acids and bases in aqueous solution, 29. IUPAC Chemical Data Series Pergamon Press, Oxford.

Plant, L., House, W., 2002. Precipitation of calcite in the presence of inorganic phosphate. Colloids and Surfaces A: Physicochemical and Engineering Aspects. 203(1): 143-153.

Plummer, L.N., Wigley, T., 1976. The dissolution of calcite in CO_2-saturated solutions at 25^0C and 1 atmosphere total pressure. Geochimica et Cosmochimica Acta. 40(2): 191-202.

Plummer, L., Wigley, T., Parkhurst, D., 1978. The kinetics of calcite dissolution in CO_2-water systems at 5^0 to 60^0C and 0.0 to 1.0 atm CO_2. American Journal of Science. 278(2): 179-216.

Pokrovsky, O.S., Golubev, S., Jordan, G., 2009a. Effect of organic and inorganic ligands on calcite and magnesite dissolution rates at 60^0C and 30 atm pCO_2. Chemical Geology. 265(1): 33-43.

Pokrovsky, O.S., Golubev, S.V., Schott, J., 2005. Dissolution kinetics of calcite, dolomite and magnesite at 25^0C and 0 to 50 atm pCO_2. Chemical Geology. 217(3): 239-255.

Pokrovsky, O.S., Golubev, S.V., Schott, J., Castillo, A., 2009b. Calcite, dolomite and magnesite dissolution kinetics in aqueous solutions at acid to circumneutral pH, 25 to 150°C and 1 to 55 atm pCO_2: New constraints on CO_2 sequestration in sedimentary basins. Chemical Geology. 265(1–2): 20-32.

Pokrovsky, O.S., Schott, J., 2001. Kinetics and mechanism of dolomite dissolution in neutral to alkaline solutions revisited. American Journal of Science. 301(7): 597-626.

Pokrovsky, O.S., Schott, J., Thomas, F., 1999. Dolomite surface speciation and reactivity in aquatic systems. Geochimica et Cosmochimica Acta. 63(19): 3133-3143.

Prochaska, C., Zouboulis, A., 2006. Removal of phosphates by pilot vertical-flow constructed wetlands using a mixture of sand and dolomite as substrate. Ecological Engineering. 26(3): 293-303.

Qing, H., Mountjoy, E., 1992. Large-scale fluid flow in the Middle Devonian Presqu'ile Barrier, Western Canada sedimentary basin. Geology. 20(10): 903-906.

Rokidi, S., Combes, C., Koutsoukos, P.G., 2011. The calcium phosphate− calcium carbonate system: growth of octacalcium phosphate on calcium carbonates. Crystal Growth & Design. 11(5): 1683-1688.

Roques, H., Nugroho-Jeudy, L., Lebugle, A., 1991. Phosphorus removal from wastewater by half-burned dolomite. Water Research. 25(8): 959-965.

Ruiz-Agudo, E., Putnis, C., 2012. Direct observations of mineral–fluid reactions using atomic force microscopy: the specific example of calcite. Mineralogical Magazine. 76(1): 227-253.

Saberi, M.R., 2010. An integrated approach for seismic characterization of carbonates. PhD Dissertation, University of Bergen. 21 p.

Sawada, K., Abdel-Aal, N., Sekino, H., Satoh, K., 2003. Adsorption of inorganic phosphates and organic polyphosphonate on calcite. Dalton Transactions(3): 342-347.

Schultheiss, S., Sethmann, I., Schlosser, M., Kleebe, H.-J., 2013. Pseudomorphic transformation of Ca/Mg carbonates into phosphates with focus on dolomite conversion. Mineralogical Magazine. 77(6): 2725-2737.

Sen, S., Pal, U., Maiti, N.C., 2014. pKa determination of d-ribose by Raman spectroscopy. The Journal of Physical Chemistry B. 118(4): 909-914.

Sharma, R.K., Chopra, S., Ray, A.K., 2014. Characterization of the dolomite reservoirs with the help of photoelectric index volume, SEG Technical Program Expanded Abstracts 2014. Society of Exploration Geophysicists, pp. 1639-1643.

Sherman, L.A., Barak, P., 2000. Solubility and dissolution kinetics of dolomite in Ca–Mg–HCO_3/CO_3 solutions at 25°C and 0.1 MPa carbon dioxide. Soil Science Society of America Journal. 64(6): 1959-1968.

Sjöberg, E.L., 1978. Kinetics and mechanism of calcite dissolution in aqueous solutions at low temperatures, Stockholm University, Stockholm: Almqvist & Wiksell, 92 pp.

Smith, R.M., Martell, A.E., 1976. Critical stability constants, vol 4, Inorganic Complexes. Plenum Press, NY.

Sø, H.U., Postma, D., Jakobsen, R., Larsen, F., 2011. Sorption of phosphate onto calcite; results from batch experiments and surface complexation modeling. Geochimica et Cosmochimica Acta. 75(10): 2911-2923.

Sulu-Gambari, F., 2011. Bacterially-induced dissolution of calcite: The role of bacteria in limestone weathering, M.Sc. thesis, McGill University, Montreal, Canada. 96p.

Suzuki, T., Inomata, S., Sawada, K., 1986. Adsorption of phosphate on calcite. Journal of the Chemical Society, Faraday Transactions 1: Physical Chemistry in Condensed Phases. 82(6): 1733-1743.

Tate, M., 1981. Determination of ionization constants by paper electrophoresis. Biochem. J. 195: 419-426.

Thomas, M.M., Clouse, J.A., Longo, J.M., 1993. Adsorption of organic compounds on carbonate minerals: 3. Influence on dissolution rates. Chemical Geology. 109(1–4): 227-237.

Tutolo, B.M., Luhmann, A.J., Kong, X.-Z., Saar, M.O., Seyfried Jr, W.E., 2014. Experimental observation of permeability changes in dolomite at CO_2 sequestration conditions. Environmental Science & Technology. 48(4): 2445-2452.

Urosevic, M., Rodriguez-Navarro, C., Putnis, C.V., Cardell, C., Putnis, A., Ruiz-Agudo, E., 2012. In situ nanoscale observations of the dissolution of dolomite cleavage surfaces. Geochimica et Cosmochimica Acta. 80: 1-13.

Verbeeck, R., De Bruyne, P., Driessens, F., Verbeek, F., 1984. Solubility of magnesium hydrogen phosphate trihydrate and ion-pair formation in the system $Mg(OH)_2$-H_3PO_4-H_2O at 25 °C. Inorganic Chemistry. 23(13): 1922-1926.

Walter, L.M., Burton, E.A., 1986. The effect of orthophosphate on carbonate mineral dissolution rates in seawater. Chemical Geology. 56(3): 313-323.

Wang, L., Li, S., Ruiz-Agudo, E., Putnis, C.V., Putnis, A., 2012. Posner's cluster revisited: direct imaging of nucleation and growth of nanoscale calcium phosphate clusters at the calcite-water interface. CrystEngComm. 14(19): 6252-6256.

Wang, T., 2012. Breakdown of the Ostwald step rule--The precipitation of calcite and dolomite from seawater at 25 and 40^0C, McGill University, Montreal, Canada, 108 pp.

Warren, J., 2000. Dolomite: occurrence, evolution and economically important associations. Earth-Science Reviews. 52(1): 1-81.

Webster, J.J., Hampton, G.J., Leach, F.R., 1984. ATP in soil: a new extractant and extraction procedure. Soil Biology and Biochemistry. 16(4): 335-342.

Wellman, T.P., Grigg, R.B., McPherson, B.J., Svec, R.K., Lichtner, P.C., 2003. Evaluation of CO_2-brine-reservoir rock interaction with laboratory flow tests and reactive transport modeling, Society of Petroleum Engineers(SPE)-80228, International Symposium on Oilfield Chemistry., Houston, Texas.

Wolicka, D., Borkowski, A., Dobrzyński, D., 2010. Interactions between microorganisms, crude oil and formation waters. Geomicrobiology Journal. 27(1): 43-52.

Xu, N., Chen, M., Zhou, K., Wang, Y., Yin, H., Chen, Z., 2014a. Retention of phosphorus on calcite and dolomite: speciation and modeling. RSC Advances. 4(66): 35205-35214.

Xu, N., Yin, H., Chen, Z., Liu, S., Chen, M., Zhang, J., 2014b. Mechanisms of phosphate retention by calcite: effects of magnesium and pH. Journal of Soils and Sediments. 14(3): 495-503.

Yoshimura, M., Sujaridworakun, P., Koh, F., Fujiwara, T., Pongkao, D., Ahniyaz, A., 2004. Hydrothermal conversion of calcite crystals to hydroxyapatite. Materials Science and Engineering: C. 24(4): 521-525.

Yuan, X., Xia, W., An, J., Yin, J., Zhou, X., Yang, W., 2015. Kinetic and thermodynamic studies on the phosphate adsorption removal by dolomite mineral. Journal of Chemistry. 2015: 1-8.

Zhang, R., Hu, S., Zhang, X., Yu, W., 2007. Dissolution kinetics of dolomite in water at elevated temperatures. Aquatic Geochemistry. 13(4): 309-338.

Figures List

Fig.10 SEM micrographs of a) fresh, ground dolomite (starting material) and recovered, reacted solids of b) control, c) monophosphate and d) AMP experiments.

Tables List

Table 1. Metal composition of the dolomite

Element	Concentration (ppm)
Calcium (Ca)	20600
Magnesium (Mg)	9260
Iron (Fe)	830
Manganese (Mn)	175
Sodium (Na)	9.2
Strontium (Sr)	53

Table 2. Chemical species considered in the speciation and equilibrium calculations.

No.	Additives	Dissolved chemical species	Acidity Constants	Stability Constants
1	Adenosine triphosphate (ATP)	*a, ATP, ATP^{1-}, ATP^{2-}, ATP^{3-}, ATP^{4-}, $ATPCa^{2-}$, $ATPMg^{2-}$, $ATPCa^{-}$, $ATPMg^{-}$	pKa1,2,3,4 = 1.8, NA, 4.0, 6.5 (*1, *2)	pK1 ($ATPCa^{2-}$) = -3.9, pK1 ($ATPMg^{2-}$) = -4.2, pK2 ($ATPCa^{-}$) = -2.1, pK2 ($ATPMg^{-}$) = -2.3 (*3)
2	Adenosine diphosphate (ADP)	*a, ADP, ADP^{1-}, ADP^{2-}, ADP^{3-}, $ADPCa^{-}$, $ADPMg^{-}$, $ADPCa^{0}$, $ADPMg^{0}$	pKa1,2,3 = 1.5, 3.9, 6.3 (*1, *2)	pK1($ADPCa^{-}$) = -2.9, pK1($ADPMg^{-}$) = -3.2, pK2($ADPCa^{0}$) = -1.6, pK2($ADPMg^{0}$) = -1.6 (*3)
3	Guanosine diphosphate (GDP)	*a, GDP, GDP^{1-}, GDP^{2-}, GDP^{3-}, $GDPCa^{-}$, $GDPMg^{-}$	pKa1,2,3 = 2.9, 6.3, 9.6 (*3)	pK($GDPCa^{-}$) = -3.4, pK($GDPMg^{-}$) = -3.4
4	Adenosine monophosphate (AMP)	*a, $C_{10}H_{14}N_5O_7P^{0}$, $C_{10}H_{13}N_5O_7P^{-}$, $C_{10}H_{12}N_5O_7P^{2-}$, $CaC_{10}H_{12}N_5O_7P^{0}$, $MgC_{10}H_{12}N_5O_7P^{0}$	pKa1,2 = 3.80, 6.23 (*3)	pK1($AMPCa^{2-}$) = -1.8, pK1($AMPMg^{2-}$) = -1.8 (*3)
5	Adenosine	*a, $C_{10}H_{13}N_5O_4$, $C_{10}H_{12}N_5O_4^{-}$, $C_{10}H_{11}N_5O_4^{2-}$, $C_{10}H_{10}N_5O_4^{3-}$	pKa1,2,3 = 3.5, NA, 12.5 (*3)	NA
6	Guanosine	*a, $C_{10}H_{13}N_5O_5$, $C_{10}H_{12}N_5O_5^{-}$, $C_{10}H_{11}N_5O_5^{2-}$, $C_{10}H_{10}N_5O_5^{3-}$	pKa1,2,3 = 2.2, 9.3, 12.4 (*3)	NA
7	Adenine	*a, $C_5H_5N_5$, $C_5H_4N_5^{-}$, $C_5H_3N_5^{2-}$, $C_5H_3N_5Ca^{0}$, $C_5H_3N_5Mg^{0}$	pKa1,2 = 4.2, 9.7 (*3)	pK($C_5H_3N_5Ca^{0}$) = -3.0, pK($C_5H_3N_5Mg^{0}$) = -3.1 (*3)

No.	Additives	Dissolved chemical species	Acidity Constants	Stability Constants
8	Guanine	*a, $C_5H_5N_5O$, $C_5H_4N_5O^-$, $C_5H_3N_5O^{2-}$, $C_5H_2N_5O^{3-}$	pKa1,2,3 = 3.3, 9.2, 12.3 (*3)	NA
9	Beta-D- Ribose	*a, $C_5H_{10}O_5$, $C_5H_9O_5^-$	pKa1 = 11.8 (*4)	NA
10	Sodium monophosphate	*a, H_3PO_4, $H_2PO_4^-$, HPO_4^{2-}, PO_4^{3-}, $CaPO_4^-$, $MgPO_4^-$	pKa1,2,3, = 2.1, 7.2, 12.4 (*5)	pK($CaPO_4^-$) = -2.2, pK($MgPO_4^-$) = -2.5 (*3)
11	Sodium diphosphate	*a, $H_4P_2O_7$, $H_3P_2O_7^-$, $H_2P_2O_7^{2-}$, $HP_2O_7^{3-}$, $P_2O_7^{4-}$, $P_2O_7Ca^{2-}$, $P_2O_7Mg^{2-}$	pKa1,2,3 = 0.8, 2.2, 6.7 (*5)	pK($P_2O_7Ca^{2-}$) = -5.0, pK($P_2O_7Mg^{2-}$) = -4.7 (*3)
12	Sodium triphosphate	*a, $H_5P_3O_{10}$, $H_4P_3O_{10}^-$, $H_3P_3O_{10}^{2-}$, $H_2P_3O_{10}^{3-}$, $HP_3O_{10}^{4-}$, $P_3O_{10}^{5-}$, $CaP_3O_{10}^{3-}$, $MgP_3O_{10}^{3-}$, $CaHP_3O_{10}^{2-}$, $MgHP_3O_{10}^{2-}$	pKa1,2,3 = 1.0, 2.0, 2.8 (*6)	pK1($CaP_3O_{10}^{3-}$) = -5.2, pK1($MgP_3O_{10}^{3-}$) = -5.8, pK2($CaHP_3O_{10}^{2-}$) = -3.0, pK2($MgHP_3O_{10}^{2-}$) = -3.5 (*3)
13	Sodium hexametaphosphate	*a, $H_6(PO_3)_6$, $H_5(PO_3)_6^-$, $H_4(PO_3)_6^{2-}$, $H_3(PO_3)_6^{3-}$, $H_2(PO_3)_6^{4-}$, $H(PO_3)_6^{5-}$, $(PO_3)_6^{6-}$, $CaP_6O_{18}^{6-}$, $MgP_6O_{18}^{6-}$	pKa1,2,3,4,5,6 = 2.0, NA, NA, NA, 5.6, 7.82(*7)	pK($CaP_6O_{18}^{4-}$) = -8.1 (*5), pK($MgP_6O_{18}^{4-}$) = -8.1 (*8)

NA- Not Available

*a- Common chemical species are H^+, OH^-, HCO_3^-, CO_3^{2-}, H_2CO_3, Ca^{2+}, $CaHCO_3^+$, $CaCO_3^0$, Mg^{2+}, $MgHCO_3^+$, $MgCO_3^0$, Na^+, $NaHCO_3^0$, $NaCO_3^-$, Cl^-

*1- (Tate, 1981), *2- (Alberty et al., 1951), *3- (Dawson et al., 1989), *4- (Sen et al., 2014), *5- (Smith and Martell, 1976)

*6- (Dai Lam et al., 2006), *7- (Perrin, 1982), *8- Assumed same value as $CaP_6O_{18}^{4-}$

Table 3. The stability constants of various calcium and magnesium phosphate species in solution at 25^0C

Species	**LogK**
$CaPO_4^-$	6.50[a,b]
$MgPO_4^-$	6.59[a]
$CaHPO_4^0$	2.74[a]
$MgHPO_4^0$	2.87[a], 2.88[c]
$CaH_2PO_4^+$	1.41[a], 1.08[b]
$MgH_2PO_4^+$	1.51[a], 1.17[c]

[a]Wateq4f.dat in Phreeqc-3.1.3.
[b]Xu et al. (2014b)
[c](Verbeeck et al. (1984)

Appendix

Tables

Table A-1. Initial and final solution pH of dissolution experiments in the absence and presence of additives (1 mM)

Additive[a]	**Initial solution pH**	**Final solution pH**
Control	5.01	5.72
Adenosine triphosphate (ATP)	4.89	5.49
Adenosine diphosphate (ADP)	4.74	5.42
Guanosine diphosphate (GDP)	4.08	5.44
Adenosine monophosphate (AMP)	4.16	5.49
Adenosine	4.28	5.76
Guanosine	4.25	5.49
Adenine	4.56	5.67
Guanine	4.54	5.71
Beta-D- Ribose	4.10	5.68
Sodium monophosphate	4.00	5.58
Sodium diphosphate	4.07	5.29
Sodium triphosphate	3.99	5.39
Sodium hexametaphosphate	4.29	5.50

[a]All experiments were conducted for 7 days at 25^0C and 1 atm pCO_2 in 300 mL of deionized water with 1mM of additive .

Table A-2. Experimental data from dolomite dissolution experiments

Experiment	RPM	Time (min)	pH	Mg:Ca molar ratio	Rate[a] (dCa/dt) ($mmolcm^{-2}\,sec^{-1}$)	Rate[a] (dMg/dt) ($mmol\,cm^{-2}\,sec^{-1}$)	Ω dolomite	log ($mHCO_3^-$)
Control	120	1440	5.54	0.89	1.5E-07	1.2E-07	3.2E-04	-2.29
		2880	5.64	0.84	7.6E-08	5.7E-08	1.6E-03	-2.18
		4320	5.67	0.81	3.4E-08	2.1E-08	2.5E-03	-2.15
		8640	5.72	0.81	1.2E-08	1.0E-08	5.0E-03	-2.09
Control+$HgCl_2$	120	380	5.20	0.78	1.6E-07	1.1E-07	4.3E-06	-2.65
		1448	5.37	0.81	6.7E-08	5.8E-08	4.9E-05	-2.47
		2880	5.45	0.81	4.0E-08	3.1E-08	1.7E-04	-2.38
		4275	5.50	0.81	2.0E-08	1.6E-08	3.1E-04	-2.33
		8665	5.57	0.82	1.3E-08	1.1E-08	9.1E-04	-2.25
ATP	120	1440	5.33	2.21	3.9E-08	6.8E-08	4.8E-06	-2.49
		2880	5.41	2.21	8.9E-09	2.0E-08	1.4E-05	-2.41
		4320	5.45	2.19	7.0E-09	1.4E-08	2.6E-05	-2.36
		5760	5.47	2.19	3.9E-09	8.3E-09	3.5E-05	-2.34
		8640	5.50	2.19	1.7E-09	3.7E-09	4.7E-05	-2.32
ATP+$HgCl_2$	120	1440	4.93	1.53	2.6E-08	4.0E-08	4.5E-08	-2.90
		2880	5.03	1.63	7.6E-09	1.5E-08	1.8E-07	-2.80
		4320	5.09	1.70	3.7E-09	8.5E-09	3.9E-07	-2.74
		5760	5.13	1.74	1.8E-09	4.8E-09	6.3E-07	-2.70
		8640	5.19	1.82	7.9E-10	2.9E-09	1.1E-06	-2.64
ADP	120	1440	5.28	1.93	3.8E-08	7.7E-08	5.0E-06	-2.55
		2880	5.34	2.02	5.9E-09	1.6E-08	1.1E-05	-2.49
		4320	5.37	1.98	3.2E-09	4.2E-09	1.6E-05	-2.46
		5760	5.40	1.94	2.4E-09	2.9E-09	2.1E-05	-2.43
		8640	5.42	1.86	2.7E-09	2.9E-09	3.1E-05	-2.40
GDP	120	1440	5.30	2.52	3.1E-08	7.7E-08	4.8E-06	-2.47
		2880	5.36	2.51	9.1E-09	2.3E-08	1.4E-05	-2.44
		4320	5.40	2.51	3.8E-09	9.7E-09	2.3E-05	-2.42
		7200	5.41	2.53	1.5E-09	4.1E-09	3.0E-05	-2.40
		8640	5.44	2.54	5.8E-10	1.6E-09	3.7E-05	-2.40
AMP	120	1440	5.39	2.57	2.1E-08	5.5E-08	5.1E-06	-2.46
		2880	5.42	2.59	3.0E-09	1.1E-08	9.4E-06	-2.42
		4320	5.43	2.60	1.9E-09	4.3E-09	1.2E-05	-2.40
		7200	5.44	2.56	1.3E-09	1.8E-09	1.4E-05	-2.40
		8640	5.50	2.50	1.3E-09	1.8E-09	2.5E-05	-2.35
Adenine	120	1440	5.50	0.79	2.2E-07	1.7E-07	4.2E-04	-2.32

Experiment	RPM	Time (min)	pH	Mg:Ca molar ratio	Rate[a] (dCa/dt) ($mmolcm^{-2}\,sec^{-1}$)	Rate[a] (dMg/dt) ($mmol\,cm^{-2}\,sec^{-1}$)	Ω dolomite	log ($mHCO_3^-$)
		2880	5.56	0.78	5.7E-08	4.3E-08	1.1E-03	-2.25
		4320	5.60	0.77	1.7E-08	1.1E-08	1.6E-03	-2.22
		5760	5.66	0.77	1.5E-08	1.1E-08	3.0E-03	-2.15
		8640	5.67	0.77	4.1E-09	4.2E-09	3.6E-03	-2.14
Adenosine	120	1440	5.63	1.05	1.7E-07	1.8E-07	1.1E-03	-2.19
		2880	5.67	1.03	1.2E-08	7.4E-09	1.6E-03	-2.16
		4320	5.69	1.00	1.3E-08	7.5E-09	2.1E-03	-2.13
		7200	5.73	0.97	9.1E-09	6.1E-09	3.5E-03	-2.09
		8640	5.76	0.96	8.4E-09	5.7E-09	4.6E-03	-2.06
Guanine	120	1440	5.46	0.79	1.8E-07	1.4E-07	2.0E-04	-2.36
		2880	5.56	0.75	5.4E-08	3.4E-08	7.2E-04	-2.26
		4320	5.62	0.76	1.3E-08	1.2E-08	1.4E-03	-2.20
		8640	5.71	0.74	2.4E-08	1.6E-08	4.8E-03	-2.09
Guanosine	120	387	5.18	0.69	1.3E-07	1.1E-07	9.8E-07	-2.54
		1518	5.40	0.78	8.1E-08	6.7E-08	4.6E-05	-2.46
		2918	5.45	0.79	2.7E-08	2.4E-08	1.1E-04	-2.43
		4345	5.49	0.78	9.6E-09	6.1E-09	1.7E-04	-2.38
		8688	5.53	0.74	8.7E-09	4.3E-09	3.1E-04	-2.35
D-ribose	120	1440	5.53	1.00	2.0E-07	2.0E-07	5.9E-04	-2.30
		2880	5.60	1.00	5.0E-08	5.0E-08	1.7E-03	-2.22
		4320	5.63	1.00	2.3E-08	2.2E-08	2.5E-03	-2.18
		5760	5.64	1.00	1.0E-08	9.6E-09	2.8E-03	-2.18
		8640	5.68	0.99	9.7E-09	9.7E-09	4.6E-03	-2.13
Hexametaphosphate	120	1440	5.39	2.74	4.2E-08	1.1E-07	1.3E-07	-2.38
		2880	5.43	2.78	6.5E-09	1.9E-09	9.7E-07	-2.34
		4320	5.47	2.79	3.5E-09	1.0E-08	2.4E-06	-2.30
		7200	5.49	2.77	2.3E-09	5.9E-09	5.2E-06	-2.28
		8640	5.50	2.76	1.7E-09	4.6E-09	6.6E-06	-2.27
Triphosphate	120	1440	5.18	2.18	3.5E-08	7.5E-08	1.3E-06	-2.63
		2880	5.26	2.27	6.1E-09	1.7E-08	3.5E-06	-2.55
		4320	5.31	2.27	4.9E-09	1.1E-08	6.6E-06	-2.50
		5760	5.33	2.27	2.7E-09	5.9E-09	9.2E-06	-2.48
		8640	5.39	2.24	1.7E-09	3.2E-09	1.8E-05	-2.41
Diphosphate	120	1440	5.09	2.42	2.5E-08	6.1E-08	4.1E-07	-2.76
		2880	5.17	2.54	3.9E-09	1.3E-08	1.2E-06	-2.67
		4320	5.22	2.49	2.7E-09	5.4E-09	2.1E-06	-2.62
		7200	5.26	2.47	2.3E-09	5.4E-09	3.9E-06	-2.58

Experiment	RPM	Time (min)	pH	Mg:Ca molar ratio	Rate[a] (dCa/dt) ($mmolcm^{-2}\,sec^{-1}$)	Rate[a] (dMg/dt) ($mmol\ cm^{-2}\,sec^{-1}$)	Ω dolomite	log ($mHCO_3^-$)
		8640	5.29	2.47	1.6E-09	4.1E-09	5.8E-06	-2.55
Monophosphate	120	1440	5.35	2.77	2.1E-08	5.9E-08	1.9E-06	-2.49
		2880	5.39	2.78	2.9E-09	1.2E-08	7.7E-06	-2.46
		4320	5.40	2.82	1.8E-09	4.8E-09	9.7E-06	-2.44
		5760	5.42	2.88	1.4E-09	3.5E-09	1.3E-05	-2.42
		8640	5.43	2.74	1.1E-09	2.3E-09	6.0E-05	-2.41
Control	30	329	5.23	0.84	2.5E-07	2.3E-07	3.9E-06	-2.62
		1466	5.51	0.84	1.1E-07	9.7E-08	2.4E-04	-2.33
		2829	5.59	0.80	5.6E-08	3.7E-08	8.2E-04	-2.23
		4179	5.62	1.00	3.0E-08	1.5E-08	1.3E-03	-2.20
		5751	5.65	0.80	1.5E-08	9.6E-09	1.9E-03	-2.17
Control	60	417	5.31	0.74	1.8E-07	1.2E-07	5.8E-06	-2.54
		1584	5.46	0.74	5.2E-08	4.4E-08	6.5E-05	-2.38
		2960	5.62	0.91	3.5E-08	2.2E-08	4.6E-04	-2.21
		4392	5.68	1.06	2.7E-08	1.7E-08	1.1E-03	-2.14
		9057	5.85	1.09	1.8E-08	1.2E-08	7.6E-03	-1.96
Control	240	365	5.35	0.82	2.4E-07	2.0E-07	1.1E-05	-2.50
		1507	5.48	0.81	7.0E-08	5.6E-08	1.1E-04	-2.36
		2900	5.57	0.82	2.9E-08	2.5E-08	3.6E-04	-2.26
		4375	5.60	0.84	2.2E-08	2.2E-08	6.7E-04	-2.22
		8995	5.69	0.78	3.2E-08	2.2E-08	3.2E-03	-2.12
Control	360	535	5.44	0.92	2.6E-07	2.4E-07	6.5E-05	-2.40
		1550	5.56	0.84	6.2E-08	4.0E-08	3.4E-04	-2.27
		3103	5.63	0.83	2.7E-08	2.2E-08	8.4E-04	-2.20
		4453	5.68	0.83	4.3E-08	3.5E-08	1.9E-03	-2.14
		10303	5.81	0.80	2.3E-08	1.7E-08	1.1E-02	-2.00

[a]The calculated rates are the means of two consecutive measurements (difference in concentration of Ca or Mg between two measurements/samplings divided by the elapsed time)

Table A-3. Saturation Index (SI) of the experimental solution with respect to various calcium phosphate phases throughout the dolomite dissolution experiment in the presence of monophosphate (1mM)

Time (min)	pH	SI (ACP)[a]	SI (HAP)[b]	SI (TCP)[c]	SI (OCP)[d]	SI (DCPD)[e]	SI (Newberyite)[f]
1440	5.26	-11.90	-5.50	-6.50	-8.08	-2.39	-2.76
2880	5.39	-11.29	-4.44	-5.89	-7.31	-2.23	-2.57
4320	5.40	-11.16	-4.22	-5.76	-7.14	-2.19	-2.56
5760	5.42	-11.02	-3.97	-5.62	-6.96	-2.15	-2.54
7200	5.53	-10.56	-3.17	-5.16	-6.39	-2.04	-2.39
8640	5.58	-10.34	-2.78	-4.94	-6.11	-1.98	-2.34

[a] K_{sp} (ACP) - 3.16×10^{-24} (Roques et al., 1991)

[b] K_{sp} (HAP, hydroxyapatite) - $Ca_5(PO_4)_3OH$ - 4.7×10^{-59} (McDowell et al., 1977)

[c] K_{sp} (TCP, tri-calcium phosphate) – $Ca_3(PO_4)_2$ - 1.26×10^{-29} (Ong et al., 2013)

[d] K_{sp} (OCP, octa-calcium phosphate) - $Ca_8H_2(PO_4)_6 \cdot 5H_2O$ - 5.01×10^{-49} (Ong et al., 2013)

[e] K_{sp} (DCPD, di-basic calcium phosphate di-hydrate) - $CaHPO_4 \cdot 2H_2O$ - 2.57×10^{-7} (Ong et al., 2013)

[f] K_{sp} (Newberyite)- $MgHPO_4 \cdot 3H_2O$ - 1.67×10^{-6} (Le Rouzic, 2013; Verbeeck et al., 1984)

where $SI = \log(\Omega) = \log(IAP/K^{o}_{sp})$

For example,

$$SI(HAP) = log\left(\frac{aCa^{5}(aPO_4)^{3}aOH}{K_{sp(HAP)}}\right) \quad \text{(A-1)}$$

References

Le Rouzic, M., 2013. Conditions de formation de la k-struvite dans les ciments phosphomagnésiens, 31ème rencontre Universitaire de l'AUGC, pp. 8p.

McDowell, H., Gregory, T., Brown, W., 1977. Solubility of $Ca_5(PO_4) \cdot 3OH$ in the system $Ca(OH)_2$-H_3PO_4-H_2O at 5, 15, 25, and 37°C. J. Res. Nat. Bur. Stand. A, 81: 273-281.

Ong, J., Appleford, M.R., Mani, G., 2013. Introduction to Biomaterials: Basic Theory with Engineering Applications. Cambridge University Press.

Roques, H., Nugroho-Jeudy, L., Lebugle, A., 1991. Phosphorus removal from wastewater by half-burned dolomite. Water Research, 25(8): 959-965.

Verbeeck, R., De Bruyne, P., Driessens, F., Verbeek, F., 1984. Solubility of magnesium hydrogen phosphate trihydrate and ion-pair formation in the system $Mg(OH)_2$-H_3PO_4-H_2O at 25 °C. Inorganic Chemistry, 23(13): 1922-1926.

Table A-4. Chemical additives supplier details and grade

Sl. No	Additives	Supplier	Chemical Grade
1	Adenosine triphosphate (ATP)	Sigma-Aldrich	99%
2	Adenosine diphosphate (ADP)	Sigma-Aldrich	> = 95 % (HPLC)
3	Adenosine Monophosphate (AMP)	Sigma-Aldrich	99%
4	Guanosine diphosphate (GDP)	Sigma-Aldrich	96 % (HPLC)
5	Adenine	Acros Organics	99 %
6	Guanine	Sigma-Aldrich	98 %
7	Beta-D- Ribose	Sigma-Aldrich	> = 98 %
8	Sodium triphosphate	Fisher Scientific	Granular/Laboratory
9	Sodium pyrophosphate	Sigma-Aldrich	> = 95 %
10	Sodium Monophosphate (ortho)	A&C American Chemical Ltd	ACS
11	Sodium Hexa metaphosphate	Sigma-Aldrich	65-70 % P_2O_5 basis
12	Adenosine	Sigma-Aldrich	> = 99 %
13	Guanosine	Acros Organics	99 %

Figures

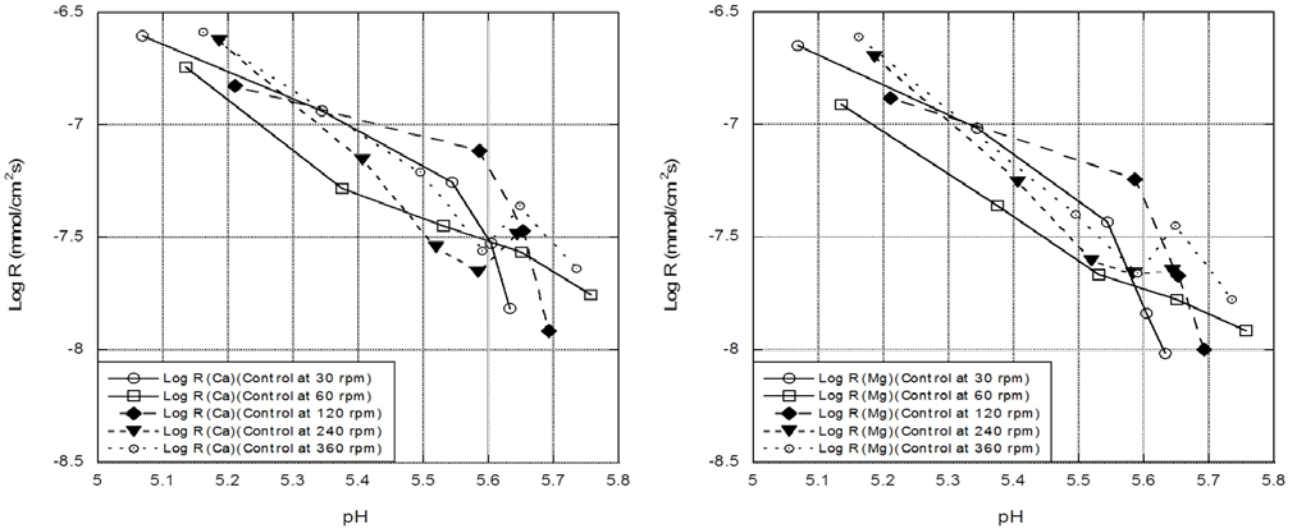

Fig.A-1 Log (rate) of dolomite dissolution rate (based on Ca and Mg release to the solution) as a function of pH at different stirring rates.